Glycosaminoglycan Overproduction in the Aorta Increases Aortic Calcification in Murine Chronic Kidney Disease

Eko Purnomo

(Degree)
博士（医学）

(Date of Degree)
2013-09-25

(Date of Publication)
2014-09-01

(Resource Type)
doctoral thesis

(Report Number)
甲第5984号

(URL)
https://hdl.handle.net/20.500.14094/D1005984

Glycosaminoglycan Overproduction in the Aorta Increases Aortic Calcification in Murine Chronic Kidney Disease

大動脈におけるグリコサミノグリカン過剰発現はマウス慢性腎障害モデルにおいて大動脈石灰化を増悪させる。

Eko Purnomo, Noriaki Emoto, Dwi Aris Agung Nugrahaningsih, Kazuhiko Nakayama, Keiko Yagi, Susi Heiden, Satomi Nadanaka, Hiroshi Kitagawa, Ken-ichi Hirata

神戸大学大学院医学研究科医科学専攻
循環器内科学
指導教員：平田健一　教授

Eko Purnomo

Key words:　Vascular calcification, Chronic kidney disease, Glycosaminoglycan, Heparan sulfate, Chondroitin sulfate

Full Title: Glycosaminoglycan Overproduction in the Aorta Increases Aortic Calcification in Murine Chronic Kidney Disease.

First Author: Eko Purnomo

Short Title: Involvement of GAG in Aortic Calcification

Authors name, academic degrees and affiliations:
Eko Purnomo, MD[1],
Noriaki Emoto, MD, PhD[1, 2],
Dwi Aris Agung Nugrahaningsih, MD, MSc.[1],
Kazuhiko Nakayama, MD, PhD[2],
Keiko Yagi, MD, PhD[2],
Susi Heiden, DVM[2],
Satomi Nadanaka, PhD[3],
Hiroshi Kitagawa, PhD[3],
Ken-ichi Hirata, MD, PhD[1]

[1]Division of Cardiovascular Medicine, Department of Internal Medicine and Division of Molecular and Cellular Biology, Kobe University Graduate School of Medicine, Kobe Japan.
[2]Department of Clinical Pharmacy, Kobe Pharmaceutical University, Kobe, Japan.
[3]Department of Biochemistry, Kobe Pharmaceutical University, Kobe, Japan.

Corresponding

Noriaki Emoto, MD, PhD.
Division of Cardiovascular Medicine, Department of Internal Medicine, Kobe University Graduate School of Medicine, 7-5-1 Kusunoki-cho, Chuo-ku, Kobe 650-0017, Japan.
Noriaki Emoto, MD, PhD.
E-mail: emoto@med.kobe-u.ac.jp
Tel: +81-78-3825846; Fax: +81-78-3825859

or

Hiroshi Kitagawa, PhD.
Department of Biochemistry, Kobe Pharmaceutical University, 4-19-1 Motoyamakita-machi, Higashinada-ku, Kobe 658-8558, Japan
E-mail: kitagawa@kobepharma-u.ac.jp.
Tel.: 81-78-441-7570; Fax: 81-78-441-7571;

Abstract

Background: Vascular calcification accompanying chronic kidney disease (CKD) increases the mortality and morbidity associated with cardiovascular disorders, but no effective therapy is available. We hypothesized that glycosaminoglycans (GAG) may contribute to osteoblastic differentiation of vascular smooth muscle cells (VSMCs) during vascular calcification.
Methods and Results: We used exostosin-like glycosyltranferase 2 deficient (EXTL2 KO) mice expressing high levels of GAG in several organs including the aorta. We performed 5/6 subtotal nephrectomy and fed the mice a high-phosphate diet to induce CKD. Overexpression of GAG in the aorta enhanced aortic calcification in CKD in EXTL2 KO mice. Ex vivo and in vitro, matrix mineralization in aortic rings and VSMCs of EXTL2 KO mice was augmented. Furthermore, removal of GAG in EXTL2 KO and WT mice-derived VSMCs effectively suppressed calcium deposition in a high-phosphate environment.
Conclusions: These results illustrate an important role for GAG in the development of vascular calcification. Manipulation of GAG expression may have beneficial effects on the progression of vascular calcification in CKD patients.

Keywords: Vascular calcification, Chronic Kidney Disease, Glycosaminoglycan, Heparan Sulfate, Chondroitin Sulfate

Non-standard Abbreviations and Acronyms

BMP	bone morphogenetic protein
BMPR	bone morphogenetic protein receptor
BUN	blood urea nitrogen
CKD	chronic kidney disease
CS	chondroitin sulfate
CSPG	chondroitin sulfate proteoglycan
GAG	glycosaminoglycan
GFR	glomerulus filtration rate
ECM	extracellular matrix
EXTL2 KO	exostosin-like glycosyltransferase 2 knockout
HPLC	high performance liquid chromatography
HS	heparan sulfate
MGP	matrix gla protein
OPN	osteopontin
Runx2	runt-related transcription factor 2
VSMCs	vascular smooth muscle cells
GlcNAc	N-acetylglucosamine

Introduction

Vascular calcification accelerates the progression of cardiovascular disorders in patients with chronic kidney disease (CKD).[1] Calcification of blood vessels reduces their elasticity and promotes arterial stiffness, increases blood and pulse pressure and the risk of heart failure.[2-4] Current therapeutic strategies for vascular calcification focus on correction of the disordered bone and mineral metabolism that accompanies CKD.[5] Vitamin D receptor agonists and calcimimetics provide survival benefits and delay the progression of vascular calcification, respectively.[6, 7] In addition, controlling the serum phosphate level using phosphate binders, sevelamer, and lanthanum offers the advantage of a low incidence of vascular calcification in CKD patients.[8, 9] However, despite the improvement of cardiovascular function and structure by sevelamer hydrochloride, other studies failed to demonstrated a significant difference in the progression of vascular calcification between calcium acetate and sevelamer hydrochloride. Furthermore, inconsistent results of sevelamer effects on mortality in HD patients have been shown in some studies.[10] Even though several potential therapies that directly ameliorate vascular calcification have presented beneficial effects in animal and human studies[11], the effects of these therapies appear to be insufficient; therefore, no effective regiment is currently available for the treatment of vascular calcification.[12] A deeper understanding of vascular calcification mechanisms is strongly necessary to provide novel strategies for the treatment of vascular calcification in CKD patients.

Vascular smooth muscle cells (VSMCs) represent the predominant cell type in the arterial walls and actively transdifferentiate into an osteoblastic/chondrocytic-like phenotype during the development of vascular calcification.[13, 14] Similar to bone cells, transdifferentiated VSMCs express osteoblastic differentiation factors such as runt-related transcription factor 2 (runx2), osteopontin (OPN), and matrix gla protein (MGP) which regulate the vascular calcification process.[15-17] Extracellular matrix (ECM) components that provide a unique environment for hydroxyapatite mineralization in bone formation[18, 19] are considered important factors in the regulation of the progression of vascular calcification. Some ECM molecules such as fibronectin and collagen I induce the in vitro calcification of vascular cells, whereas other molecules such as collagen IV inhibit this process.[20] Accumulation of proteoglycans, another ECM component, in intimal and medial calcification is associated with atherosclerotic plaques as well as calcified nodules in the aortic valve, suggesting that proteoglycans are involved in the development of vascular calcification. [21-23]

Heparan sulfate (HS) and chondroitin sulfate (CS) are glycosaminoglycan (GAG) chains expressed at the cell surface and in the extracellular matrix, and modulate various aspects of physiologic and pathologic conditions.[24-26] These molecules are composed of repeated disaccharide units of N-acetylated hexosamine and hexuronic acid that covalently bind to the core protein of proteoglycans through a tetrasaccharide linkage. Sulfation of N-acetylated hexosamine and hexuronic acid provides negative charges that enable the binding of ligands.[25-28] The ubiquitous expression of these molecules in various tissues, particularly blood vessels, suggests a contribution to vascular development as well as the progression of vascular diseases.[29-31] Given their roles in osteogenesis[32-36], GAGs may contribute to the osteoblastic differentiation of VSMCs during vascular calcification. However, few studies have addressed the role of GAG modification in the progression of vascular calcification in CKD.

To evaluate the role of GAGs in aortic calcification, we used exostosin-like glycosyltransferase 2 deficient (EXTL2 KO) mice, which overexpress GAGs.[37] The mice were subjected to 5/6 subtotal nephrectomy and administered a high-phosphate diet to induce CKD. In this study, we also demonstrated the involvement of GAGs in vascular calcification

through ex vivo and in vitro studies using aortic rings and VSMCs of EXTL2 KO mice, respectively. Our study provides evidence that increased GAG expression in murine aortas in CKD augments aortic calcification. In addition, deletion of GAG in VSMCs effectively attenuates in vitro calcification.

Material and methods

1. Animal Studies

The Animal Research and Ethics Committee of Kobe Pharmaceutical University, Kobe, Japan approved all our animal procedures. In this study, we used EXTL2 KO mice (n=23) and their wild-type (WT) littermates (n=25) that were previously generated.[37] Both strains were maintained on a C57BL/6 genetic background. Male mice aged 8-10 weeks were anesthetized with sodium pentobarbital and subjected to 5/6 sub total nephrectomy with 2 steps surgery procedure, as described previously (EXTL2 KO n=15; EXTL2 WT mice n=16).[38] Sham operated mice were used as control (EXTL2 KO mice n=8; EXTL2 WT mice n=9). After completion of the 5/6 sub total nephrectomy, mice received high-phosphate diet containing 1.5% phosphate (termed as CKD groups). Sham-operated groups received normal-phosphate diet containing 0.5% phosphate (termed as control groups) (MF high phosphate diet and MF normal diet (Oriental Yeast Co. Ltd., Osaka, Japan)). Mice were sacrificed after 8 weeks of diet administration.

2. Systemic Parameters

Mouse body weight was measured before and at the end of experiment. Systemic blood pressure was determined by tail-cuff methods system (Softron, Tokyo, Japan) following the acclimatization procedure in conscious mice and repeating 10 times measurement for each mouse. Using metabolic cages, one day prior to sacrifice date, urine was collected. In the end of experiment, blood was taken by cardiac puncture. Blood urea nitrogen (BUN), and serum phosphate were analyzed by urease-GLDH method and enzymatic fluorimetric assay for glucose-6-phosphate, respectively. Serum and urine creatinine were measured by enzymatic assay (Nescoat VLII CRE kit, Alfresa Pharma Corporation, Osaka, Japan). Glomerulus Filtration Rate (GFR) was estimated by measuring the mouse creatinine clearance. Aortic tissue was prepared for calcium measurement, RNA, and histological examinations. Thoracic aorta was used for histology samples and abdominal aorta was used for calcium and RNA measurement.

3. In vitro and ex vivo calcification

Mouse VSMCs were isolated from aorta of control animals (3 mice for each genotype), as previously described.[39] Briefly, aorta was isolated and dissected from the fibrous and lipid tissue in the surrounding area. In the sterile culture medium, aorta was cut in to small pieces approximately 1-2 mm on side, and then incubated with type 2 collagenase at 37 ˚C for 6 hours. VSMCs were detached from the tissue by flicking gently, transferred and incubated in 48 well culture dishes, then leaved undisturbed for 5 days. Cells with passage number 3-10 were used for experiment. Cells were culture with DMEM high glucose (WAKO, Osaka, Japan), containing 15% FBS (Biowest, Nuaillé, France), 1% (v/v) penicillin/streptomycin/amphotericin B (Wako, Osaka, Japan), 1 mM sodium pyruvate (Gibco Invitrogen Corporation, New York, USA) until 90-100% confluence then treated with high phosphate medium (phosphate inorganic (Pi) = 3 mM) or normal medium (Pi = 0.9 mM) as the normal control for 6 days. Medium was changed every other day. Heparitinase (EC 4.2.2.8, 10 mIU/ml) and chondroitinase ABC from Proteus vulgaris (EC 4.2.2.4, 20 mIU/ml) were added to remove HS and CS from the cell surface of VSMCs. Three separated wells

were used for each group of treatment. For ex vivo calcification, the dissected thoracic aorta was cut in to small rings with a length of approximately 4-5 mm and cultured with a normal or high phosphate medium for 6 days. Four aortas from four different control mice were used for each group of treatment.

4. Calcium quantification

Aortic and cellular calcium were extracted in the 200 µl of HCl 0.6 M at 4˚C for 24 hours, and transferred into new tube for calcium quantification. Aortic, cellular, and serum calcium level were determined by o-Cresophtalein Complexone (Sigma-Aldrich, Missouri, USA) and commercial detection reagents, according to manufacture's protocol. Protein was extracted from aortic samples and cells by incubation with 10% NaOH and 1% SDS, and then subjected to protein concentration measurement. The aortic calcium content (µg) was standardized using aortic dry weight (mg). In vitro and ex vivo calcium amount (µg) was standardized based on the protein content (mg).

5. Quantitative real-time PCR

Messenger RNA was extracted by TRIzole reagent (Gibco Invitrogen Corporation, New York, USA). The extracted RNA was digested with RQ1 RNase-free DNase and stop solution (Promega, Wisconsin, USA) for 30 minute at 37˚C and 10 min at 65˚C, respectively. Reverse transcriptase PCR was performed by using Murine-Moloney Leukemia Virus Reverse Transcriptase (Gibco Invitrogen Corporation, New York, USA) with random primers (Takara bio Inc., Shiga, Japan). Quantitative real-time PCR was performed using Fast Start DNA Master plus SYBR Green I and a LightCycler 1.5 (Roche Applied Science, Indianapolis, USA) according to the manufacturer's procedures. The primers are:

- mouse matrix gla protein (MGP):
  - forward primer : ccg aga cac cat gaa gag c
  - reverse primer : gat tcg tag cac agg gttg
- mouse osteopontin (OPN) :
  - forward primer : ccc ggt gaa agt gac tga t
  - reverse primer : ttc ttc aga gga cac agc att c
- mouse bone morphogenetic protein 2 (BMP2) :
  - forward primer : atg taa tca gaa gaa ata tcg ggt
  - reverse primer : gga ctt gaa ctt gtg aac ttt aac
- mouse BMP receptor type Ia (BMPRIa) :
  - forward primer : cca tta tag aag aag atg atc agg g
  - reverse primer : ctg caa ata ctg gtt gca c
- mouse BMP receptor type II (BMPRII) :
  - forward primer : agg cag cca aca tag tg
  - reverse primer : agg cag cca aca tag tg
- mouse glyceraldehyde-3-phosphate dehydrogenase (GAPDH)
  - forward primer : cat ctg agg gcc cac tg
  - reverse primer : gag gcc atg tag gcc atg a

6. Immunohistochemistry and histology

Aortic tissue was fixed in the 4 % paraformaldehyde in PBS (phosphate-buffered saline) (v/v) at 4 ˚C for overnight. The fixated aorta was subjected to paraffin or frozen block preparation. Four µm slides were used for hematoxyllin-eosin staining and immunohistochemistry. After performing antigen retrieval step using citrate buffer, the samples were permeabilized using 0.05% triton X-100 in PBS (v/v) and blocked in the 5% BSA (bovine serum albumin) in PBS (v/v). The primary antibodies are anti heparan sulfate

antibody, HepSS-1, anti chondroitin sulfate antibody, 3B3, 1:100 (Seikagaku Biobusiness Corporation, Tokyo, Japan), anti phosphorylated (p)-smad1/5/8 antibody 1:100, anti smooth muscle (SM)-22α antibody 1:100 (Cell Signaling Technologies, Massachusetts, USA), anti α-Smooth Muscle Actin (SMA)-FITC antibody 1:100 (Sigma Aldrich Corporation, Missouri, USA), anti Runx2 antibody, 1:100 (Santa Cruz Biotechnology Inc., Texas, USA). After adequate washing step, the samples sections were incubated with appropriate secondary antibodies. Images were captured with an LSM 710 laser-scanning confocal microscope using a 20x objective. Overt matrix mineralization and calcium deposition in the mouse aorta and VSMCs were detected by Von Kossa staining and alizarin red, respectively.

7. GAG fluorescent labeling and immunocytochemistry.

Mouse VSMCs were fixed in 4% PFA in PBS (v/v). Fixated cells were permeabilized in 0.05% Triton X-100 in PBS (v/v) prior to blocking with 5% BSA in PBS (v/v). HepSS-1 and CS56 primary antibodies (Sigma Aldrich Corporation, Missouri, USA) were used for labeling the heparan sulfate and chondroitin sulfate, respectively. To observe apoptosis process, anti Caspase 3 antibody (Santa Cruz Biotechnology Inc., Texas, USA) was used. After incubation with the appropriate secondary antibodies, images were captured using an LSM 710 laser-scanning confocal microscope with a 10x objective.

8. Proliferation and migration assays

To examine the proliferation activity of VSMCs, the cell proliferation reagent WST-1 was used according to manufacture's protocol. Briefly, VSMCs (4×10^3 cells / well) were culture to 50% confluence. The cells were treated with medium containing 15 % fetal bovine serum. The chondroitinase ABC and heparitinase were added to the well of enzymes treated group. Cells with free serum medium were used as a control. After 24 hours incubation, 10 µl WST-1 reagent were added to each well and the cells were re-incubated for another 2 hours. The color intensity was read at 450 nm (reference wavelength 655nm). To measure migration activity, we used scratch wound assay as described previously.[40] VSMCs were seeded into 6 well dishes. Confluent monolayers were scraped through the middle of the dish by using a modified 100µl tip. After wounding, monolayers were immediately washed with DMEM and incubated with 15% FBS. Heparitinase and chondroitinase ABC were added in enzymes treated group. After 48 hours, wound closure area from the wound edge was quantified.

9. BMP2 accumulation assay in aortic tissue

Recombinant human BMP2 (rhBMP2) (R&D systems, Minnesota, USA) (1 µg/mL) was pre-incubated with goat anti-polyclonal BMP2 (Santa Cruz Biotechnology Inc., Texas, USA) (2 µg/mL) at 37°C for 30 minutes. Fixed aortic tissue was incubated with the ligand-antibody complex at 4°C for 30 min. Following incubation, the aortic tissues were washed with PBS and blocked using 5% BSA at room temperature for 30 min. The aortic samples were incubated in donkey anti-goat Alexa Fluor 488-conjugated secondary antibody. Fluorescence was visualized using an LSM 710 laser-scanning confocal microscope with a 20× objective.

10. Disaccharide composition analysis in aortic tissue

The aorta was harvested from 8-wk-old male mice (3 mice for each genotype), homogenized in cold acetone, and evaporated overnight. The resulting dry powder was digested by actinase E at 55°C for 24 h. The digested sample was resuspended in 5% trichloroacetic acid and centrifuged, and the supernatant was extracted using diethyl ether. The aqueous phase was neutralized and precipitated using 80% ethanol. The precipitate was dissolved in pyridine acetate buffer and subjected to filtration on a PD-10 column (GE Healthcare, Buckinghamshire, UK). The flow-through products were evaporated and the dried samples

were digested using a mixture of heparitinase (EC 4.2.2.8, 1 mIU) and heparinase (EC 4.2.2.7, 1 mIU) from Flavobacterium heparinum or chondroitinase ABC from Proteus vulgaris (EC 4.2.2.4, 10 mIU) at 37°C for 4 h. The digested GAGs were derivatized using the fluorophore 2-aminobenzamide and then analyzed by high-performance liquid chromatography (HPLC) - SLC-10A system (Shimadzu, Kyoto, Japan) on a PA-03 column (YMC, Kyoto, Japan) as reported previously.[41]

11. Statistical analysis

Results are presented as the mean ± SEM. The data distribution was tested using Kolmogorov-Smirnov test. Normally distributed variables were analysed using ANOVA followed with Unpaired Student's t-test. Variables not normally distributed were analyzed using non-parametric analysis with Kruskal Wallis followed by Mann Whitney U test. All analyses were performed using GraphPad Prism software (GraphPad, California, USA). Differences were considered significant when $p < 0.05$.

Results

Augmented GAG chains (HS and CS) in aortas of EXTL2 KO mice

The disaccharide content of GAG chains (HS and CS) in the aortas of EXTL2 KO mice was higher than that in the aortas of WT mice (Table 1 and 2). We also examined disaccharides composition on those mice and found that 6-sulfation pattern composition of CS in EXTL2 KO mice is higher compared with in EXTL2 WT mice.

Equal development of CKD in EXTL2 KO and WT mice following 5/6 subtotal nephrectomy and high-phosphate diet administration

To determine the presence of CKD, BUN and GFR were measured in EXTL2 KO and WT mice. In both CKD groups, the kidney function was markedly reduced, as demonstrated by higher BUN and lower GFR (Figure 1A and 1B). No significant difference between the 2 genotypes was observed under normal conditions. As expected, the high-phosphate diet in the CKD group induced high serum phosphate levels, with no effect on serum calcium levels; thus, the serum Ca x P product was increased in both genotypes (Figure 1C-E). The mouse body weight decreased in all CKD groups, and a lower body weight was detected in EXTL2 KO mice (Figure 2A). SBP levels were elevated in EXTL2 KO mice suffering from CKD (Figure 2B).

Increased aortic calcification in aortas of EXTL2 KO mice with CKD

Reduced renal function and high phosphate levels contribute to the development of aortic calcification. We determined the aortic calcification by qualitative and quantitative method, which are Von Kossa staining and aortic calcium content measurement, respectively. We used Von Kossa staining to show overt calcification. We found that Von Kossa staining was positive only in 5 out of 15 of EXTL2 KO mice in CKD condition, which mean 30% of the mice in this group showed overt calcification (Figure 3A-H). Calcification was mainly visible in the media layer of aorta, within and surrounding elastic fibers; this layer predominantly consists of vascular smooth muscle cells. All other experimental groups did not show overt signs of calcification. Furthermore, to measure the extent of aortic calcification; we measured calcium content in aorta. Even tough, not all EXTL2 KO mice under CKD showed overt calcification; the average of the calcium content in this group is the highest among all groups (Figure 3M). To confirm that HS and CS chains are important for aortic calcification, isolated aortic rings from control mice of both genotypes were cultured in normal or high-phosphate medium. As shown in Figure 3N, although the high-phosphate medium elevated the calcium

deposition in both genotypes, the aorta of EXTL2 KO mice demonstrated significantly higher calcium deposition than that of WT mice.

Alterations in bone matrix components and vascular smooth muscle cell markers in the calcified aorta of EXTL2 KO mice.

Immunostaining revealed a high expression of the osteoblastic differentiation markers Runx2 (Figure 4E–M) and type Ia collagen (Figure 5E-M) in the calcified aorta of EXTL2 KO mice, but little or no expression in the other groups. Concomitant with the calcium deposition in the aorta, the mRNA level of MGP increased in the EXTL2 KO mice with calcified aortas compared to that in WT mice with CKD, and the other control groups (Figure 6A). Similarly, the OPN mRNA level was up-regulated in the calcified aorta of EXTL2 KO mice (Figure 6B). In addition, calcified aorta of EXTL2 KO mice demonstrated a loss of vascular smooth muscle cell markers such as SM22- α and α-SMA (Figure 7).

CKD increases HS and CS levels in calcified and non-calcified aortas

The accumulation of extracellular matrix components in calcified lesions is considered to stimulate subsequent vascular calcification. In the present study, HS and CS levels were much higher in the calcified aortas of CKD-induced EXTL2 KO mice than in the aortas of control EXTL2 KO mice, which already showed an up-regulation of HS and CS in their aortas. HS and CS levels were also increased in the non-calcified aortas of CKD-induced WT mice (Figure 8).

Attenuation of HS or CS expression decreases calcium deposition in VSMCs cultured in high-phosphate conditions

Heparitinase and chondroitinase treatment effectively reduced heparan sulfate and chondroitin sulfate expression in cell surface of VSMCs, respectively (Figure 9). These treatments have no significant effects on proliferation, migration, and apoptosis activity in treated VSMCs (Figure 10). Under high-phosphate treatment, alizarin red staining and calcium quantification revealed matrix mineralization in mouse VSMCs (Figure 11). In support of the in vivo results, EXTL2 KO VSMCs that overexpressed HS and CS demonstrated higher calcium deposition (1/3-fold increase) under the high-phosphate condition than those from WT mice. To investigate which GAG contributed to vascular calcification, removal of HS or CS by enzymatic digestion was performed in vitro in high phosphate-containing mouse VSMCs. Heparitinase treatment effectively decreased the amount of alizarin red staining and the calcium level in high-phosphate-induced mouse VSMCs. Furthermore, treatment with chondroitinase also markedly reduced matrix mineralization and calcium deposition in high phosphate-containing EXTL2 KO and WT mouse VSMCs.

Up-regulation of BMP2 signaling in the calcified aorta

Many studies have shown that BMP2 signaling positively contributes to osteoblastic differentiation of VSMCs during vascular calcification. In the present study, we observed that BMP2 mRNA was increased in both CKD groups. No difference was observed in the expression of BMPR Ia and BMPR II. P-Smad1/5/8 expression downstream of BMP signaling was only detected clearly in the calcified aortas of EXTL2 KO mice (Figure 12). In addition, extracellular BMP2 accumulated to a greater extent in the calcified aorta than in the WT aorta (Figure 13).

Discussion

In this study, we demonstrate that the overexpression of HS and CS contributes to vascular calcification in CKD in vivo. We also confirmed the involvement of HS and CS in vascular calcification by ex vivo and in vitro studies. Under high phosphate condition, the calcium deposition was increased in aortic tissue samples and aortic VSMCs derived from EXTL2 KO mice compared to those from WT mice. Furthermore, deletion of HS or CS in mouse VSMCs decreased the amount of calcium deposition. These findings suggest that HS and CS enhanced the vascular calcification progression in high phosphate condition.

To evaluate the involvement of HS and CS in vascular calcification, we used EXTL2 KO mice, which show elevated HS and CS expression. EXTL2 is an enzyme involved in HS and CS biosynthesis; in particular, it has transferase activity, and mediates the transfer of the first N-acetylglucosamine (GlcNAc) via an α1, 4 linkage to a phosphorylated tetrasaccharide core region, which results in the termination of HS and CS.[25, 37, 42] Deletion of EXTL2 in mice disturbs this process and permits the accumulation of HS and CS in vivo. EXTL2 KO mice show an increased HS and CS expression in the liver, brain, and embryonic fibroblasts.[37] In the present study, we also observed high HS and CS expression in the aorta of these mice. HS and CS were clearly expressed in the aorta, particularly in the sub-endothelial and medial layers. It is likely that the lack of EXTL2 in mice did not affect their growth process, as they grew normally and had normal blood pressure under physiologic conditions. In addition, there is no study reported about the role of EXTL2 and other EXT's families beyond regulation of GAG biosynthesis. Therefore, we considered that the excess GAG expression in the EXTL2 KO mouse might contribute during pathologic condition particularly in the vascular calcification development. Supporting our study, current report by Nadanaka et al. showed the important role of EXTL2 mediated GAG synthesis in regenerating process during liver injury.[43] Regarding our hypothesis that GAG overproduction might have deleterious effects during vascular calcification, we used mice of the C7BL/6J strain that are relatively resistant to vascular calcification[44], which favor us to evaluate the role of HS and CS in enhancing vascular calcification.

The severity of CKD has important role in the development of vascular calcification. Therefore, we examined the kidney function in all comparable group mice. However, we observed that kidney functions did not differ between EXTL2 KO and WT mice, under either normal conditions or following CKD induction. Considering the importance of phosphate in the development of vascular calcification, we also examined the serum phosphate concentration in all treatment groups. We found that the phosphate concentration was not affected by genotypic differences. Systolic blood pressure was initially similar among all the treatment groups. In our study, EXTL2 KO mice did not develop aortic calcification spontaneously. Interestingly, after 2 months of CKD with high phosphate condition, we found that EXTL2 KO mice clearly showed more vascular calcification than WT mice and observed that those mice developed higher systolic blood pressure than WT mice. We assume that vascular calcification, which is accompanied by increased stiffness and decreased compliance of arteries[45, 46], increased systolic blood pressure. From these results, we suggest that overproduction of GAG in EXTL2 KO mice enhanced the aortic calcification under CKD with high phosphate condition.

To support the in vivo finding that demonstrate the GAG role in vascular calcification, we also did ex vivo study using aortic ring and in vitro study using aortic VSCMs which are isolated from control mice of both EXTL2 KO and WT mice. Our ex vivo study showed that aortic ring tissue from EXTL2 KO mice has higher calcium deposition than that from WT mice in the presence of high-phosphate medium. In vitro study showed that VSMCs of EXTL2 KO mice under high phosphate medium have higher calcium deposition than those of

other groups. Futhermore, we also showed that deletion HS and CS using heparitinase and chondroitinase, respectively result in lowering the calcium deposition under high phosphate conditions. These results confirmed that over expressed GAG might contribute in aortic calcification under high phosphate conditions.

Previous studies suggested that proteoglycan contributes to the progression of vascular calcification. Decorin, a chondroitin sulfate proteoglycan (CSPG), was found at sites of calcification within the aortic valve[23] and atherosclerotic plaque of human coronary arteries.[21] Increased decorin expression promotes in vitro calcification of VSMCs.[21] In addition, other CSPGs, biglycan, and versican were expressed in calcified nodules and areas surrounding calcified lesions in the aortic valve, which suggests that biglycan and versican actively induce and modulate soft tissue mineralization, respectively.[23] However, these studies provide no evidence for the contribution of HS and CS to vascular calcification. Our study suggests that accumulation of HS and CS in the mice aorta contributes to matrix mineralization in the aorta. The negative charges of sulfate residue in HS and CS create ligand-binding sites and modulate their activity. The most well-known growth factor ligand related to osteoblastic differentiation is BMP2. By acting as a co-receptor for BMP2, HS accelerates the formation of a complex between BMP2 and BMP receptors, and contributes to enhance BMP2 signaling.[27] HS modulates the distribution of BMP2 on the cell surface, prolongs the half-life of BMP2, and reduces the interaction of BMP2 with its antagonist.[34] In a human study, Koleganova et al. observed that BMP2 expression was higher in the aorta of CKD patients than in controls, but no difference was found between calcified and non-calcified aortas.[47] Consistent with this study, we observed higher level of BMP2 in CKD mice than control mice. However, we did not observe any difference in BMP2 and BMPR receptor expression in both CKD groups. Interestingly, p-smad1/5/8 activation was detected higher in the calcified aortas of EXTL2 KO mice than aorta of other groups. These results suggested that overproduction of HS might mediate the BMP2 binding with BMP receptors and activate the signal transduction. To visualize BMP2 distribution in aortic tissue, we performed BMP2 accumulation assays and found that BMP2 was more abundantly accumulated in calcified aortas than in tissues from other groups. It is likely that high HS and CS levels in CKD contribute to the attachment of BMP2 to BMP receptors and the activation of downstream signaling. Activation of BMP2 signaling has been further shown to affect the phenotypic transition of VSMCs[48]. Similarly; we detected high expression of Runx2, an osteoblastic differentiation factor, and low expression of the VSMC markers SM22-α and α-SMA in the calcified aorta. These findings suggest that under high phosphate condition, high HS and CS levels in the aortas of EXTL2 KO mice accelerate vascular calcification by enhancing BMP2 signaling through p-smad1/5/8, which further induces phenotypic transition of VSMCs.

In addition, previous studies showed that sulfation pattern of GAG contributes in the various mechanisms.[49, 50] In our study, we also measured the disaccharides composition and found that the 6-sulfation pattern but not 4-sulfation of CS in EXTL2 KO mice is higher compare to those on EXTL2 WT mice but. During osteoblastic differentiation, CS-C, which consists of 6-O-sulfate at its N-acetylated hexosamine and hexuronic acid residues, activates p-smad1/5/8 expression. However, CS-E, which is enriched with 4-O-sulfate and 6-O-sulfate at its N-acetylated hexosamine and hexuronic acid residues, activates p-smad1/5/8 expression with higher level than CS-C.[36] Despite the modest role of 6-sulfation during osteoblast differentiation, the change of disaccharides composition in EXTL2 KO mice may also contribute in the vascular calcification development. Nevertheless, further study is needed to elucidate the importance of 6-sulfation pattern during vascular calcification development.

In the in vitro study, we demonstrated that under high phosphate condition, overexpression of GAG enhanced calcium deposition in mouse VSMCs and deleting the cell surface and extracellular matrix HS or CS from mouse VSMCs effectively abrogated the

calcification.

In conclusion, we are the first to demonstrate the importance of HS and CS in CKD-induced vascular calcification. Up-regulation of HS and CS in aortic tissue clearly accelerates the progression of vascular calcification in animals with CKD. Attenuation of HS or CS effectively reduces the calcium deposition in VSMCs under high phosphate condition. Considering the complexity of vascular calcification mechanisms, a balance between vascular calcification inducers and inhibitors is necessary. These results suggest that controlling HS and CS expression may help in preventing or inhibiting the progression of vascular calcification in CKD.

Source of Funding

This study was supported by following grants:

- Ministry of Education, Culture, Sports, Science, and Technology (MEXT)-supported Program for the Strategic Research Foundation at Private Universities, 2012–2017 (to H. K.)
- The Science Research Promotion Fund from The Promotion and Mutual Aid Corporation for Private Schools of Japan (to N.E).
- Grant-in-Aid for Scientific Research in Innovative Areas 23110003 (Deciphering Sugar Chain-based Signals Regulating Integrative Neuronal Functions (to H. K.)) from MEXT, Japan.
- Faculty Resources Grant, Kobe University, the Global COE Program, Global Center of Excellence for Education and Research on Signal Transduction Medicine in the Coming Generation from the Ministry of Education, Culture, Sports, Science, and Technology (MEXT) of Japan (to E.P).

Disclosures

None

References

1. Herzog CA, Asinger RW, Berger AK, Charytan DM, Diez J, Hart RG, Eckardt KU, Kasiske BL, McCullough PA, Passman RS, DeLoach SS, Pun PH, Ritz E. Cardiovascular disease in chronic kidney disease. A clinical update from Kidney Disease: Improving Global Outcomes (KDIGO). Kidney Int. 2011; 80:572-586.
2. Aoki A, Kojima F, Uchida K, Tanaka Y, Nitta K. Associations between vascular calcification, arterial stiffness and bone mineral density in chronic hemodialysis patients. Geriatr Gerontol Int. 2009; 9:246-252.
3. Jensky NE, Criqui MH, Wright MC, Wassel CL, Brody SA, Allison MA. Blood pressure and vascular calcification. Hypertension. 2010; 55:990-997.
4. Miwa Y, Tsushima M, Arima H, Kawano Y, Sasaguri T. Pulse pressure is an independent predictor for the progression of aortic wall calcification in patients with controlled hyperlipidemia. Hypertension. 2004; 43:536-540.
5. O'Neill WC, Lomashvili KA. Recent progress in the treatment of vascular calcification. Kidney Int. 2010; 78:1232-1239.
6. Wolf M, Shah A, Gutierrez O, Ankers E, Monroy M, Tamez H, Steele D, Chang Y, Camargo CA Jr, Tonelli M, Thadhani R. Vitamin D levels and early mortality among incident hemodialysis patients. Kidney Int. 2007; 72:1004-1013.
7. Raggi P, Chertow GM, Torres PU, Csiky B, Naso A, Nossuli K, Moustafa M, Goodman WG, Lopez N, Downey G, Dehmel B, Floege J. The ADVANCE study: a randomized study to evaluate the effects of cinacalcet plus low-dose vitamin D on vascular

calcification in patients on hemodialysis. Nephrol Dial Transplant. 2011; 26: 1327-1339
8. Takei T, Otsubo S, Uchida K, Matsugami K, Mimuro T, Kabaya T, Akiba T, Nitta K. Effects of sevelamer on the progression of vascular calcification in patients on chronic haemodialysis. Nephron Clin Pract. 2008; 108: 278-283.
9. Hutchison AJ, Smith CP, Brenchley PE. Pharmacology, efficacy and safety of oral phosphate binders. Nat Rev Nephrol. 2011; 7: 578-589.
10. Ikee R, Tsunoda M, Sasaki N, Sato N, Hashimoto N. Emerging effects of sevelamer in chronic kidney disease. Kidney Blood Press Res. 2013; 37:24-32.
11. Wu M, Rementer C, Giachelli CM. Vascular Calcification: An Update on Mechanisms and Challenges in Treatment. Calcif Tissue Int. 2013; 1:1-9
12. Checherita IA, Smarandache D, David C, Ciocalteu A, Ion DA, Lascar I. Vascular calcifications in chronic kidney disease-clinical management. Rom J Morphol Embryol. 2012; 53:7-13.
13. Bostrom K, Watson KE, Horn S, Wortham C, Herman IM, Demer LL. Bone morphogenetic protein expression in human atherosclerotic lesions. J Clin Invest. 1993; 91:1800-1809.
14. Speer MY, Yang HY, Brabb T, Leaf E, Look A, Lin WL, Frutkin A, Dichek D, Giachelli CM. Smooth muscle cells give rise to osteochondrogenic precursors and chondrocytes in calcifying arteries. Circ Res. 2009; 104:733-741.
15. Steitz SA, Speer MY, Curinga G, Yang HY, Haynes P, Aebersold R, Schinke T, Karsenty G, Giachelli CM. Smooth muscle cell phenotypic transition associated with calcification: upregulation of Cbfa1 and downregulation of smooth muscle lineage markers. Circ Res. 2001; 89:1147-1154.
16. Chen NX, O'Neill KD, Duan D, Moe SM. Phosphorus and uremic serum up-regulate osteopontin expression in vascular smooth muscle cells. Kidney Int. 2002; 62:1724-1731.
17. Lomashvili KA, Wang X, Wallin R, O'Neill WC. Matrix Gla protein metabolism in vascular smooth muscle and role in uremic vascular calcification. J Biol Chem. 2011; 286:28715-28722.
18. Veis A. Mineral-matrix interactions in bone and dentin. J Bone Miner Res. 1993; 8:493-497.
19. McQuillan DJ, Richardson MD, Bateman JF. Matrix deposition by a calcifying human osteogenic sarcoma cell line (SAOS-2). Bone. 1995; 16:415-426.
20. Watson KE, Parhami F, Shin V, Demer LL. Fibronectin and collagen I matrixes promote calcification of vascular cells in vitro, whereas collagen IV matrix is inhibitory. Arterioscler Thromb Vasc Biol. 1998; 18:1964-1971.
21. Fischer JW, Steitz SA, Johnson PY, Burke A, Kolodgie F, Virmani R, Giachelli C, Wight TN. Decorin promotes aortic smooth muscle cell calcification and colocalizes to calcified regions in human atherosclerotic lesions. Arterioscler Thromb Vasc Biol. 2004; 24:2391-2396.
22. Luo G, Ducy P, McKee MD, Pinero GJ, Loyer E, Behringer RR, Karsenty G. Spontaneous calcification of arteries and cartilage in mice lacking matrix GLA protein. Nature. 1997; 386:78-81.
23. Stephens EH, Saltarrelli JG, Baggett LS, Nandi I, Kuo JJ, Davis AR, Olmsted-Davis EA, Reardon MJ, Morrisett JD, Grande-Allen KJ. Differential proteoglycan and hyaluronan distribution in calcified aortic valves. Cardiovasc Pathol. 2011; 20:334-342.
24. Bishop JR, Schuksz M, Esko JD. Heparan sulphate proteoglycans fine-tune mammalian physiology. Nature. 2007; 446:1030-1037.
25. Nadanaka S, Kitagawa H. Heparan sulphate biosynthesis and disease. J Biochem. 2008; 144:7-14.

26. Afratis N, Gialeli C, Nikitovic D, Tsegenidis T, Karousou E, Theocharis AD, Pavao MS, Tzanakakis GN, Karamanos NK. Glycosaminoglycans: key players in cancer cell biology and treatment. FEBS J. 2012; 279:1177-1197.
27. Kuo WJ, Digman MA, Lander AD. Heparan sulfate acts as a bone morphogenetic protein coreceptor by facilitating ligand-induced receptor hetero-oligomerization. Mol Biol Cell. 2010; 21:4028-4041.
28. Hu Z, Wang C, Xiao Y, Sheng N, Chen Y, Xu Y, Zhang L, Mo W, Jing N, Hu G. NDST1-dependent heparan sulfate regulates BMP signaling and internalization in lung development. J Cell Sci. 2009; 122:1145-1154.
29. Adhikari N, Carlson M, Lerman B, Hall JL. Changes in expression of proteoglycan core proteins and heparan sulfate enzymes in the developing and adult murine aorta. J Cardiovasc Transl Res. 2011; 4:313-320.
30. Tran-Lundmark K, Tran PK, Paulsson-Berne G, Friden V, Soininen R, Tryggvason K, Wight TN, Kinsella MG, Boren J, Hedin U. Heparan sulfate in perlecan promotes mouse atherosclerosis: roles in lipid permeability, lipid retention, and smooth muscle cell proliferation. Circ Res. 2008; 103:43-52.
31. Wight TN, Merrilees MJ. Proteoglycans in atherosclerosis and restenosis: key roles for versican. Circ Res. 2004; 94:1158-1167.
32. Duncan GC, McCormick, Tufaro F. The link between heparan sulfate and hereditary bone disease: finding a function for the EXT family of putative tumor suppressor proteins. J Clin Invest. 2001; 108:511-516.
33. Cortes M, Baria AT, Schwartz NB. Sulfation of chondroitin sulfate proteoglycans is necessary for proper Indian hedgehog signaling in the developing growth plate. Development. 2009; 136:1697-1706.
34. Bramono DS, Murali S, Rai B, Ling L, Poh WT, Lim ZX, Stein GS, Nurcombe V, van Wijnen AJ, Cool SM. Bone marrow-derived heparan sulfate potentiates the osteogenic activity of bone morphogenetic protein-2 (BMP-2). Bone. 2012; 50:954-964.
35. Buttner M, Keller M, Huster D, Schiller J, Schnabelrauch M, Dieter P, Hempel U. Over-sulfated chondroitin sulfate derivatives induce osteogenic differentiation of hMSC independent of BMP-2 and TGF-beta1 signalling. J Cell Physiol. 2013; 228:330-340.
36. Koike T, Izumikawa T, Tamura J, Kitagawa H. Chondroitin sulfate-E fine-tunes osteoblast differentiation via ERK1/2, Smad3 and Smad1/5/8 signaling by binding to N-cadherin and cadherin-11. Biochem Biophys Res Commun. 2012; 420:523-529.
37. Nadanaka S, Zhou S, Kagiyama S, Shoji N, Sugahara K, Sugihara K, Asano M, Kitagawa H. EXTL2, a member of EXT family of tumor suppressors, controls glycosaminoglycan biosynthesis in a xylose kinase-dependent manner. J Biol Chem. 2013; 288:9321-9333.
38. Miyazaki-Anzai S, Levi M, Kratzer A, Ting TC, Lewis LB, Miyazaki M. Farnesoid X receptor activation prevents the development of vascular calcification in ApoE-/- mice with chronic kidney disease. Circ Res. 2010; 106:1807-1817.
39. Ray JL, Leach R, Herbert JM, Benson M. Isolation of vascular smooth muscle cells from a single murine aorta. Methods Cell Sci. 2001; 23:185-188.
40. DeBiasio R, Bright GR, Ernst LA, Waggoner AS, Taylor DL. Five-parameter fluorescence imaging: wound healing of living Swiss 3T3 cells. J Cell Biol. 1987; 105:1613-1622.
41. Okada M, Nadanaka S, Shoji N, Tamura J, Kitagawa H. Biosynthesis of heparan sulfate in EXT1-deficient cells. Biochem J. 2010; 428:463-471.
42. Wuyts W, Van Hul W, Hendrickx J, Speleman F, Wauters J, De Boulle K, Van Roy N, Van Agtmael T, Bossuyt P, Willems PJ. Identification and characterization of a novel member of the EXT gene family, EXTL2. Eur J Hum Genet. 1997; 5:382-389.

43. Nadanaka S, Kagiyama S, Kitagawa H. EXTL2, a member of EXT family of tumor suppressors, in liver injury and regeneration processes. Biochem J. 2013; 454:133-145
44. Qiao JH, Xie PZ, Fishbein MC, Kreuzer J, Drake TA, Demer LL, Lusis AJ. Pathology of atheromatous lesions in inbred and genetically engineered mice. Genetic determination of arterial calcification. Arterioscler Thromb. 1994; 14:1480-1497.
45. McEniery CM, McDonnell BJ, So A, Aitken S, Bolton CE, Munnery M, Hickson SS, Yasmin, Maki-Petaja KM, Cockcroft JR, Dixon AK, Wilkinson IB. Aortic calcification is associated with aortic stiffness and isolated systolic hypertension in healthy individuals. Hypertension. 2009; 53:524-531.
46. Rattazzi M, Bertacco E, Puato M, Faggin E, Pauletto P. Hypertension and vascular calcification: a vicious cycle? J Hypertens. 2012; 30:1885-1893.
47. Koleganova N, Piecha G, Ritz E, Schirmacher P, Muller A, Meyer HP, Gross ML. Arterial calcification in patients with chronic kidney disease. Nephrol Dial Transplant. 2009; 24:2488-2496.
48. Li X, Yang HY, Giachelli CM. BMP-2 promotes phosphate uptake, phenotypic modulation, and calcification of human vascular smooth muscle cells. Atherosclerosis. 2008; 199:271-277.
49. Miyata S, Komatsu Y, Yoshimura Y, Taya C, Kitagawa H. Persistent cortical plasticity by upregulation of chondroitin 6-sulfation. Nat Neurosci. 2012; 15:414-422.
50. Garg HG, Yu L, Hales CA, Toida T, Islam T, Linhardt RJ. Sulfation patterns in heparin and heparan sulfate: effects on the proliferation of bovine pulmonary artery smooth muscle cells. Biochim Biophys Acta. 2003; 1639:225-231.

TABLE LEGENDS

TABLE 1

Aorta of EXTL2 KO mice contains higher HS amounts than those of WT mice. Disaccharide composition of HS from aorta of 8 weeks old male mice. Data are shown as pmol of disaccharide per mg of acetone powder of aorta, the mean ± S.E.M, and percentage from total amount of three independent experiments.
* $p < 0.05$ vs WT mice by Unpaired Student's t-test.

TABLE 2

Aorta of EXTL2 KO mice contains higher CS amounts than those of WT mice. Disaccharide composition of CS from aorta of 8 weeks old male mice. Data are shown as pmol of disaccharide per mg of acetone powder of aorta, the mean ± S.E.M, and percentage from total amount of three independent experiments.
* $p < 0.05$ vs WT mice by Unpaired Student's t-test.

FIGURE LEGENDS

FIGURE 1

Development of CKD that represented by serum chemistry was independent from genotype of all groups. (A) All mice under CKD groups have higher blood urea nitrogen (BUN), reaching two folded differences than control groups. **(B)** In addition, both EXTL2 KO and WT mice in CKD groups have lower glomerular filtration rate (GFR) approximately 50% less than in the control groups. **(C)** Mice with CKD condition show significantly higher serum phosphate than control groups. **(D)** However, serum calcium concentration was determined in same level in all-comparable groups. **(E)** The product of serum calcium x phosphate was higher in CKD groups than control groups. Data are shown as mean ± S.E.M ($n = 3$-6) * $p < 0.05$, ** $p < 0.01$; BUN, serum phosphate, and serum calcium by Unpaired Student's t-test; GFR and serum Ca x P product by Mann Whitney U test.

FIGURE 2

Chronic kidney disease influenced body weight and blood pressure after 2 months treatment. (A) After 2 months treatment, marked weight loss was found in all CKD groups. Besides, EXTL2 KO mice have lower body weight than WT mice. **(B)** CKD induced EXTL2 KO mice have remarkably higher systolic blood pressure than its control and WT mice. Data are shown as mean ± S.E.M ($n = 7$-9), * $p < 0.05$, ** $p < 0.01$, *** $p < 0.005$ by Unpaired Student's t-test .

FIGURE 3

Deleting EXTL2 gene aggravated aortic calcification under CKD. (A-H) Calcium deposition (black color) visualized by Von Kossa staining was predominantly in the aortic media. **(I-L)** Aortic structure was shown by hematoxylin and eosin staining. **(M)** Quantification of calcium content in the mice aorta has shown that EXTL2 KO mice under CKD developed more calcium deposition than WT mice (Control group, $n = 5$-6; CKD group, $n = 15$-16). Data are shown as mean ± S.E.M, * $p < 0.05$, ** $p < 0.01$ by Mann Whitney U test. **(N)** Calcium deposition quantification in aortic culture of EXTL2 KO and WT mice after 6 days phosphate treatment ($n = 5$ separated mice). Data are shown as mean ± S.E.M, *** $p < 0.005$ by Unpaired Student's t-test .

FIGURE 4

Enhancement of Runx2 in EXTL2 KO mice aorta. (A-D) Serial section of each group was detected by Von Kossa staining. **(E-L)** Runx2, which is related with osteoblastic differentiation, was enhanced in the calcified aorta of EXTL2 KO mice. **(M)** Quantification result of Runx2 signal per aortic area. Data are shown as mean ± S.E.M (n = 6), * $p < 0.05$ by Mann Whitney U test.

FIGURE 5

Augmentation of collagen Ia in calcified aorta of EXTL2 KO mice. (A-D) Serial section of each group was detected by Von Kossa staining. **(E-L)** Collagen Ia was up-regulated in calcified aorta of EXTL2 KO mice. **(M)** Quantification result of collagen Ia signal in aortic area. Data are shown as mean ± S.E.M (n = 6), *** $p < 0.005$ by Unpaired Student's t-test .

FIGURE 6

Enhancement of bone matrix components in EXTL2 KO mice aorta. (A,B) Quantitative real time PCR results show an up regulation of MGP and OPN in calcified aorta. Data are shown as mean ± S.E.M (n = 4-6). * $p < 0.05$ by Mann Whitney U test.

FIGURE 7

Vascular smooth muscle cells loss in calcified aorta of EXTL2 KO mice. . **(A-D)** Serial section of each group was detected by Von Kossa staining. **(E-L)** α-SMA and **(M-T)** SM22-α as contractile phenotype markers of VSMC were highly expressed in both control groups and CKD group of WT mice. However, their expression was attenuated in calcified aorta of EXTL2 KO mice under CKD condition. Quantification result of α-SMA **(U)** and SM22-α **(V)** signal in aortic area. Data are shown as mean ± S.E.M (n = 6), * $p < 0.05$, ** $p < 0.01$, *** $p < 0.005$ by Unpaired Student's t-test .

FIGURE 8

Heparan sulfate and chondroitin sulfate signals were increased in CKD treated group. (A-D) Serial section of each group was detected by Von Kossa staining. HS and CS expression in mice aorta were detected by HepSS-1 **(E-L)** and 3B3 **(Q-X)** antibody, respectively. Their expression were up-regulated under CKD. HepSS-1 and 3B3 signal was quantified and shown as percentage per aortic area (**Y** and **Z**, respectively). Data are shown as mean ± S.E.M (n = 6). * $p < 0.05$, ** $p < 0.01$, *** $p < 0.005$ by Unpaired Student's t-test .

FIGURE 9

Heparan sulfate and chondroitin sulfate expression was reduced under enzymes treatment. (A, B, E, F) Heparan sulfate expression and **(C, D, G, H)** chondroitin sulfate expression was reduced after heparitinase and chondroitinase treatment, respectively. HepSS-1 and CS56 signal were quantified and shown as percentage per measured area (**I** and **J**, respectively). Data are shown as mean ± S.E.M (n = 6). *** $p < 0.005$ by Unpaired Student's t-test .

FIGURE 10

Proliferation, migration, and apoptosis activity are not affected by enzymes treatment. (A) Proliferation and **(B)** Migration activity of both genotypes VSMCs were not significantly different and not affected by heparitinase or chondroitinase treatment. **(C)** Caspase 3 expression was in the similar level in all treated groups. Data are shown as mean ± S.E.M (n = 3) by Mann Whitney U test.

FIGURE 11

Removal of HS and CS cell surface structure ameliorated calcium deposition of high phosphate treated VSMCs. (A, B, E, F) Alizarin red positive area was markedly up regulated in phosphate treated cells and extensive positive area was found in EXTL2 KO mouse VSMCs. **(C, G)** Removal of HS by using heparitinase 10 mIU/ml effectively attenuated calcium deposition under high phosphate condition. **(D, H)** Chondroitin sulfate digestion by chondroitinase 20 mIU/ml treatment also decreased the amount of calcium deposition in high phosphate treatment. **(I)** Calcium deposition was quantified by o-Cresophtalein Complexone method in all comparable groups. Data are presented as mean ± S.E.M (n = 3). * $p < 0.05$, $\delta < 0.001$, *f* $p < 0.0005$, # $p < 0.0001$ by Unpaired Student's t-test .

FIGURE 12

Activated BMP signaling in calcified aorta of EXTL2 KO mice. Phosphorylated-smad 1/5/8 was enhanced in calcified aorta of EXTL2 KO mice **(H, L)** but not in other groups **(E-G, I-K)**. P-smad 1. 5, 8 signal was quantified and shown as percentage per aortic area **(M)** The mRNA expression of BMP2 ligands determined by qRT-PCR showed increased in both CKD groups. However, no significant different of BMP2 expression in CKD groups was found **(N).** We observed no differences in both BMP receptor type Ia (BMPRIa) and BMP receptor type II (BMPRII) **(O and P).** Data are presented as mean ± S.E.M (n = 4-5). *$p < 0.05$**,** **$p < 0.001$, n.s. = not siginificant by Mann Whitney U test.

FIGURE 13. BMP2 accumulation in calcified aorta. Exogenous rhBMP2 was more abundantly trapped on calcified aorta **(H, L)** than WT CKD and both control groups **(E - G, I - K)**.

TABLE 1
Disaccharide composition of HS from aorta of EXTL2 KO or WT mice

Composition	Aorta {pmol/mg (mol %)}	
	EXTL2 KO	WT
Δ DiHS-0S	464.6 ± 70.7 (38.4)	239.8 ± 70.7 (38.4)
Δ DiHS-6S	35.3 ± 13.7 (3.1)	28.5 ± 13.4 (4.6)
Δ DiHS-NS	535.2 ± 67.0 (46.4)	266.5 ± 43.1 (42.7)
Δ DiHS-diS_1	21.9 ± 7.2 (1.9)	12.7 ± 4.6 (2.0)
Δ DiHS-diS_2	82.2 ± 6.6 (7.1)	69.2 ± 16.9 (11.1)
Δ DiHS-TriS	14.5 ± 3.5 (1.3)	7.5 ± 3.8 (1.2)
Total	1153.8 ± 209.2 (100)*	624.4 ± 139.6 (100)

Abbreviations:
ΔDiHS-0S, ΔHexUA α1-4GlcNAc; ΔDiHS-6S, ΔHexUA α1-4GlcNAc(6S); ΔDiHS-NS, ΔHexUA α1-4GlcNS; ΔDiHS-diS_1, ΔHexUA α1-4Glc(NS,6S); ΔDi-diS_2, ΔHexUA(2S) α1-4GlcNS; ΔDi-triS, ΔHexUA(2S) α1-4Glc(NS,6S)

TABLE 2
Disaccharides composition of CS from aorta of EXTL2 KO and WT mice

Composition	Aorta {pmol/mg (mol %)}	
	EXTL2 KO	WT
Δ DiCS-0S	138.2 ± 57.8 (18.7)	123.5 ± 50.1 (25.4)
Δ DiCS-6S	257.9 ± 33.7 (34.8)*	121.5 ± 26.8 (25.0)
Δ DiCS-4S	332.2 ± 112.1 (44.8)	234.3 ± 70.0 (48.2)
Δ DiCS-diSD	12.4 ± 2.9 (1.7)	6.4 ± 1.9 (1.3)
Δ DiCS-diSE	ND	ND
Δ DiCS-TriS	ND	ND
Total	740 ± 145.5 (100)*	485.7 ± 145.4 (100)

Abbreviations:
ΔDi-0S, ΔHexUA α1-3GalNAc; ΔDi-6S, ΔHexUA α1-3GalNAc (6S); ΔDi-4S, ΔHexUA α1-3GalNAc(4S); ΔDi-diSD, ΔHexUA(2S) α1-3GalNAc(6S); ΔDi-diSE, ΔHexUA α1-3GalNAc(4S,6S); ΔDi-triS, ΔHexUA(2S) α1-3GalNAc(4S,6S); ND, not detected.

FIGURE 1

A

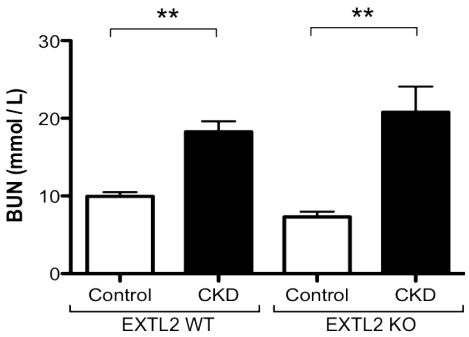

B

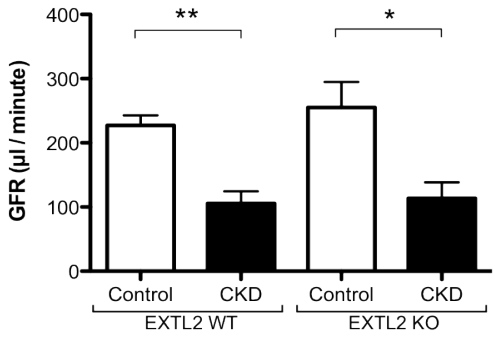

C

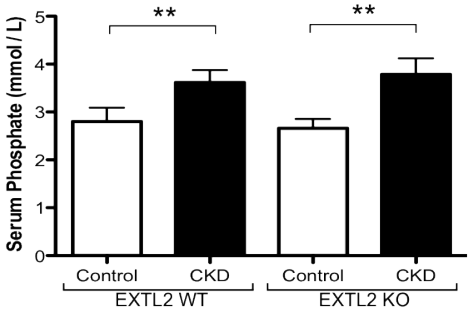

D

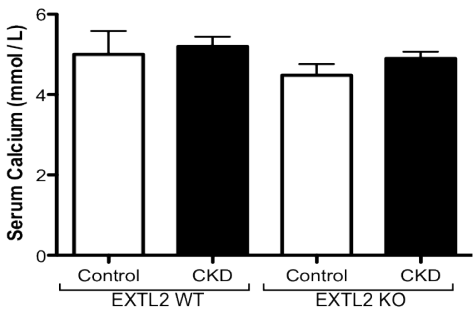

E

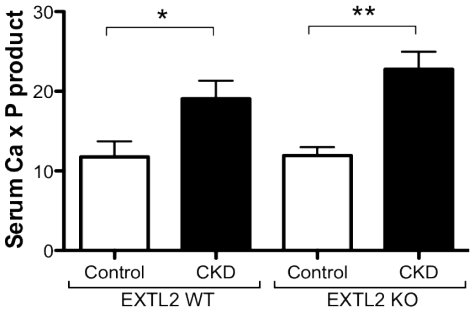

FIGURE 2

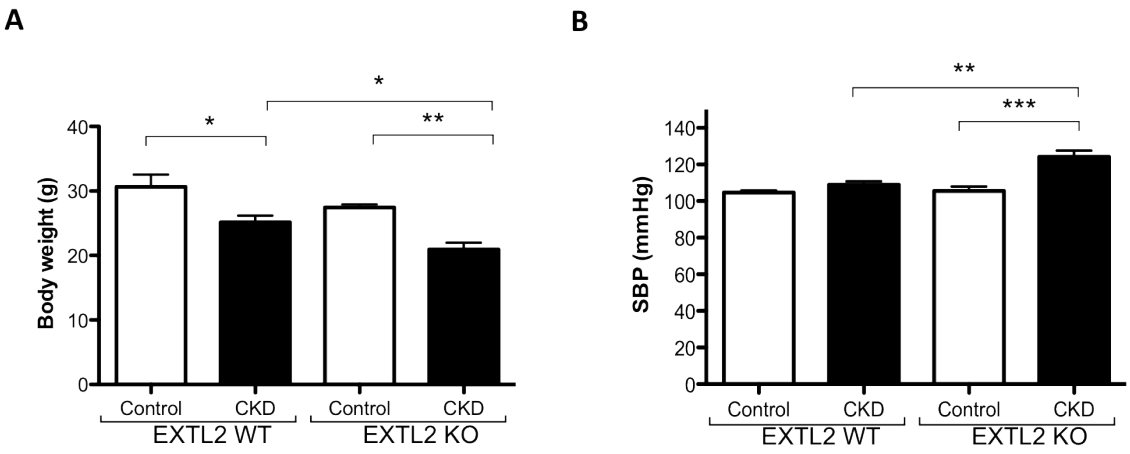
A
B
Body weight (g)
40
30
20
10
0
*
*
**
Control
CKD
Control
CKD
EXTL2 WT
EXTL2 KO
SBP (mmHg)
140
120
100
80
60
40
20
0
**
***
Control
CKD
Control
CKD
EXTL2 WT
EXTL2 KO

FIGURE 3

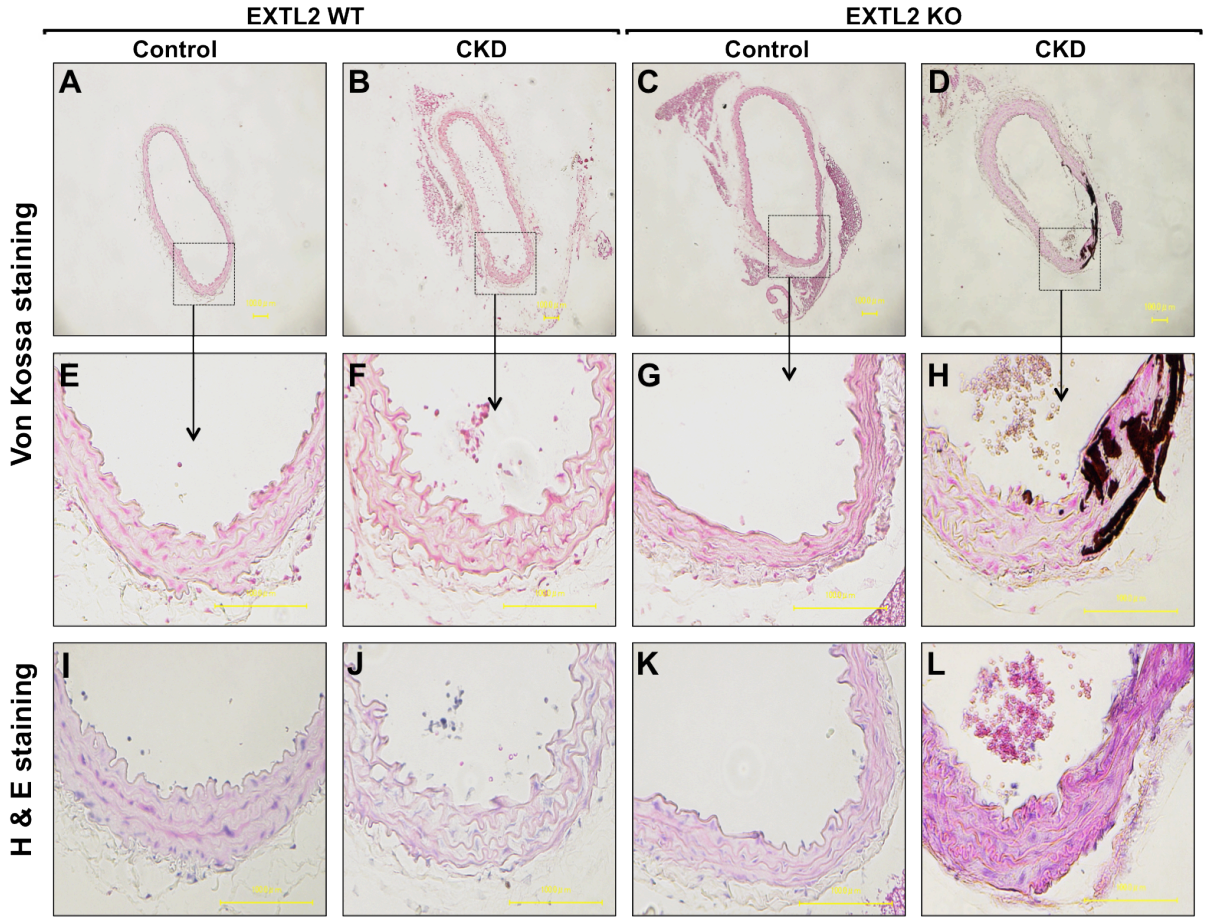
EXTL2 WT
EXTL2 KO
Control
CKD
Control
CKD
Von Kossa staining
H & E staining
A
B
C
D
E
F
G
H
I
J
K
L

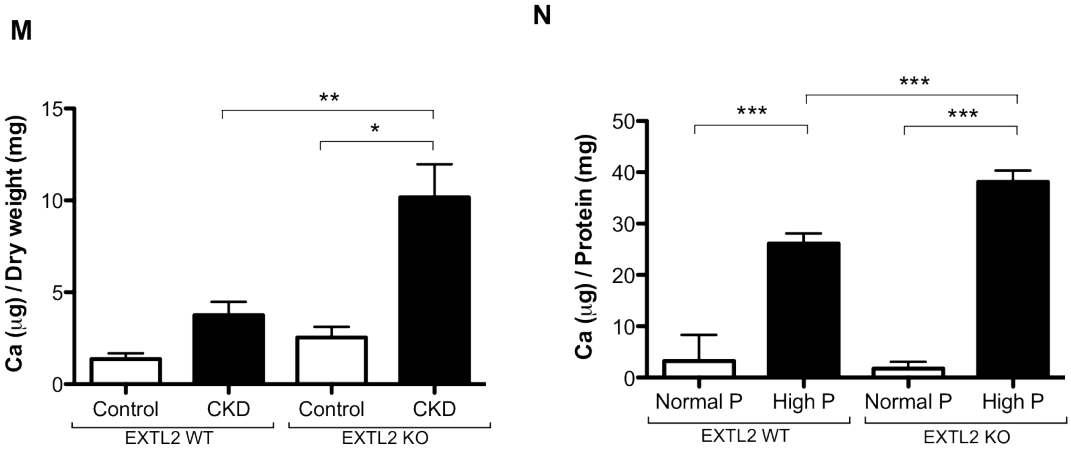
M
Ca (μg) / Dry weight (mg)
15
10
5
0
**
*
Control
CKD
Control
CKD
EXTL2 WT
EXTL2 KO
N
Ca (μg) / Protein (mg)
50
40
30
20
10
0
***
***
***
Normal P
High P
Normal P
High P
EXTL2 WT
EXTL2 KO

FIGURE 4

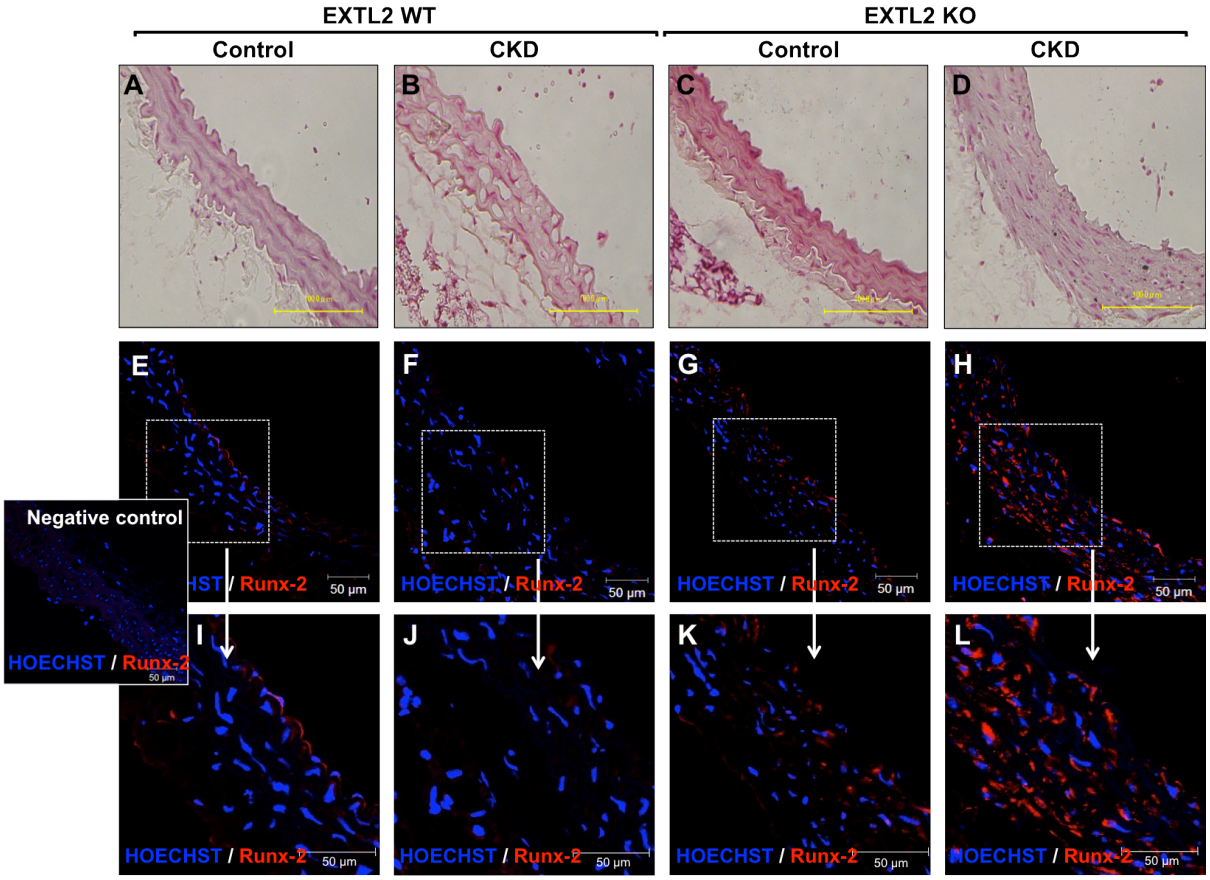
EXTL2 WT
EXTL2 KO
Control
CKD
Control
CKD
A
B
C
D
E
F
G
H
Negative control
HOECHST / Runx-2
50 µm
I
J
K
L

M

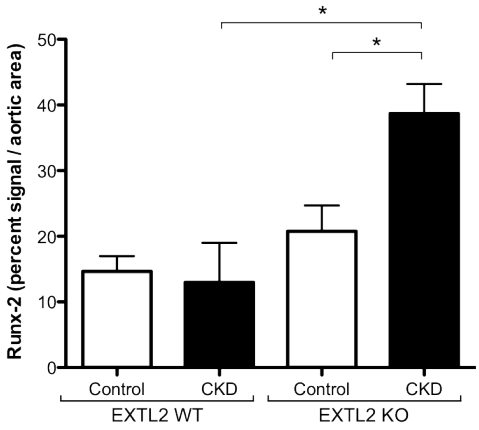
Runx-2 (percent signal / aortic area)
50
40
30
20
10
0
*
*
Control
CKD
Control
CKD
EXTL2 WT
EXTL2 KO

FIGURE 5

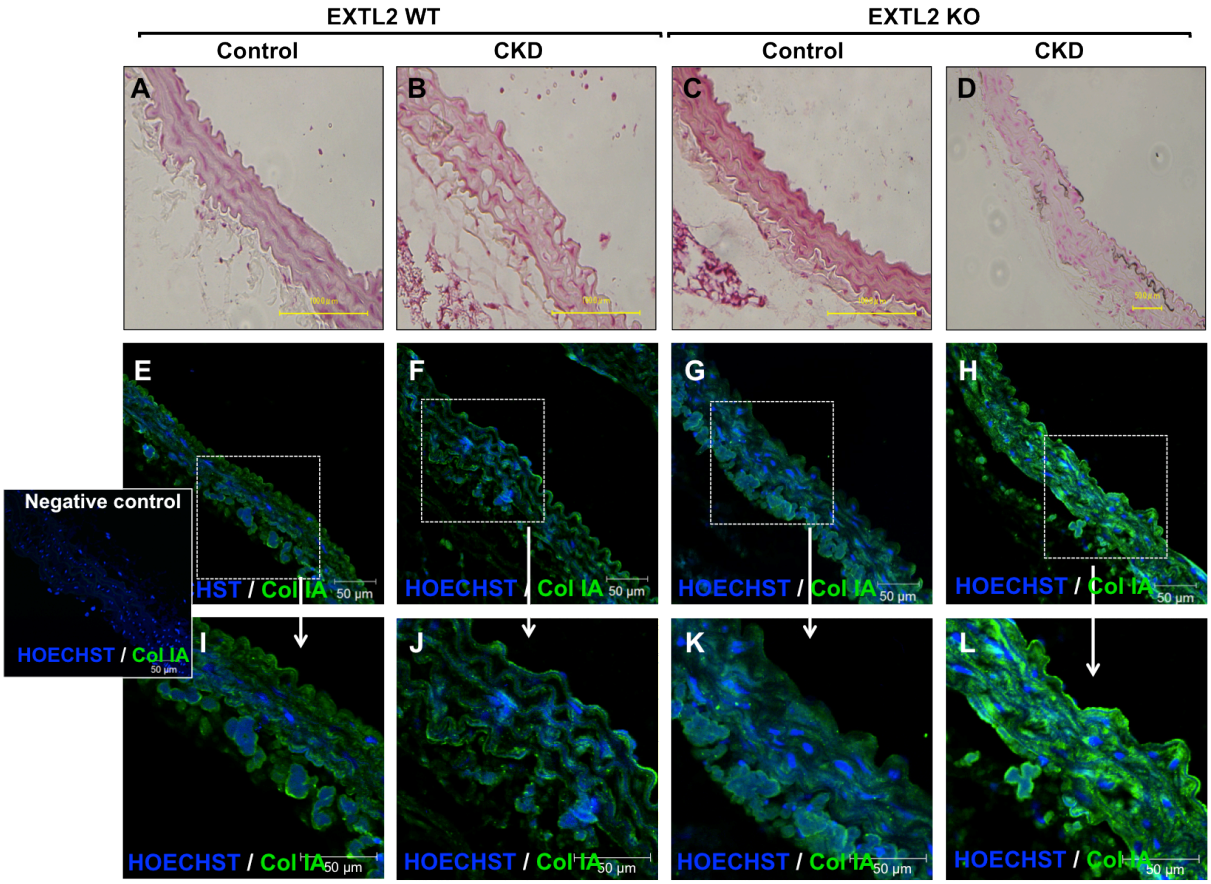
EXTL2 WT
EXTL2 KO
Control
CKD
Control
CKD
A
B
C
D
E
F
G
H
Negative control
HOECHST / Col IA
50 µm
I
J
K
L

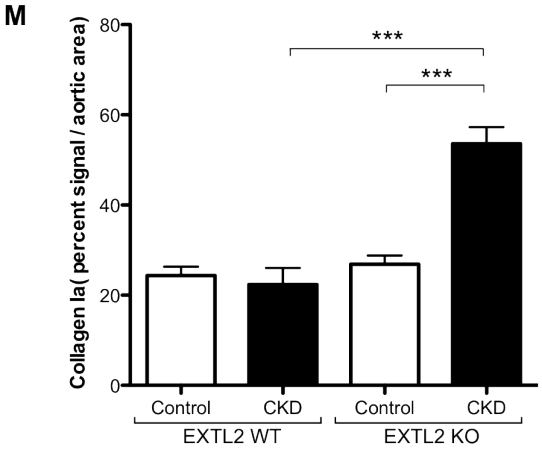
M
Collagen Ia (percent signal / aortic area)
80
60
40
20
0
***
***
Control
CKD
Control
CKD
EXTL2 WT
EXTL2 KO

FIGURE 6

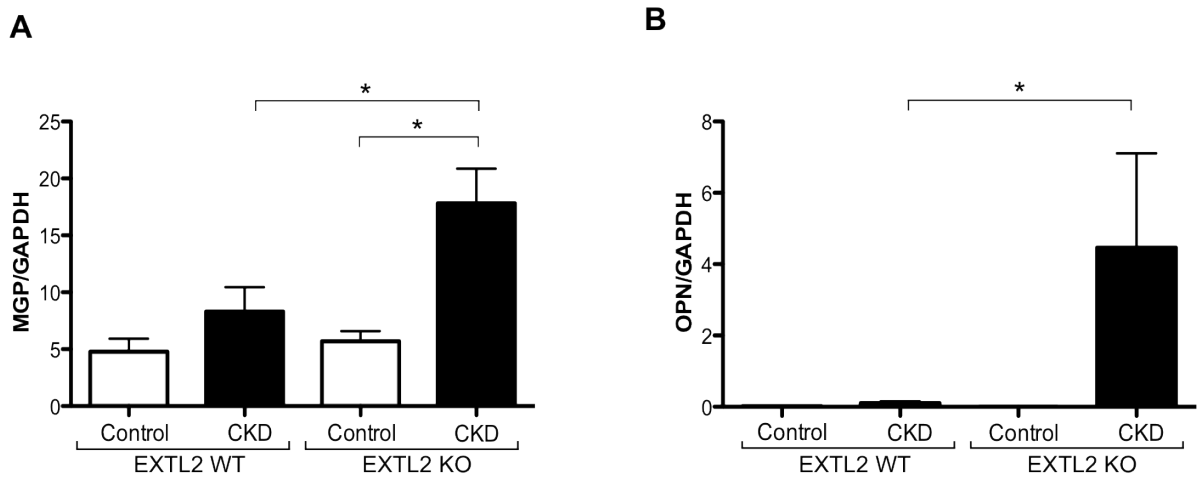

FIGURE 7

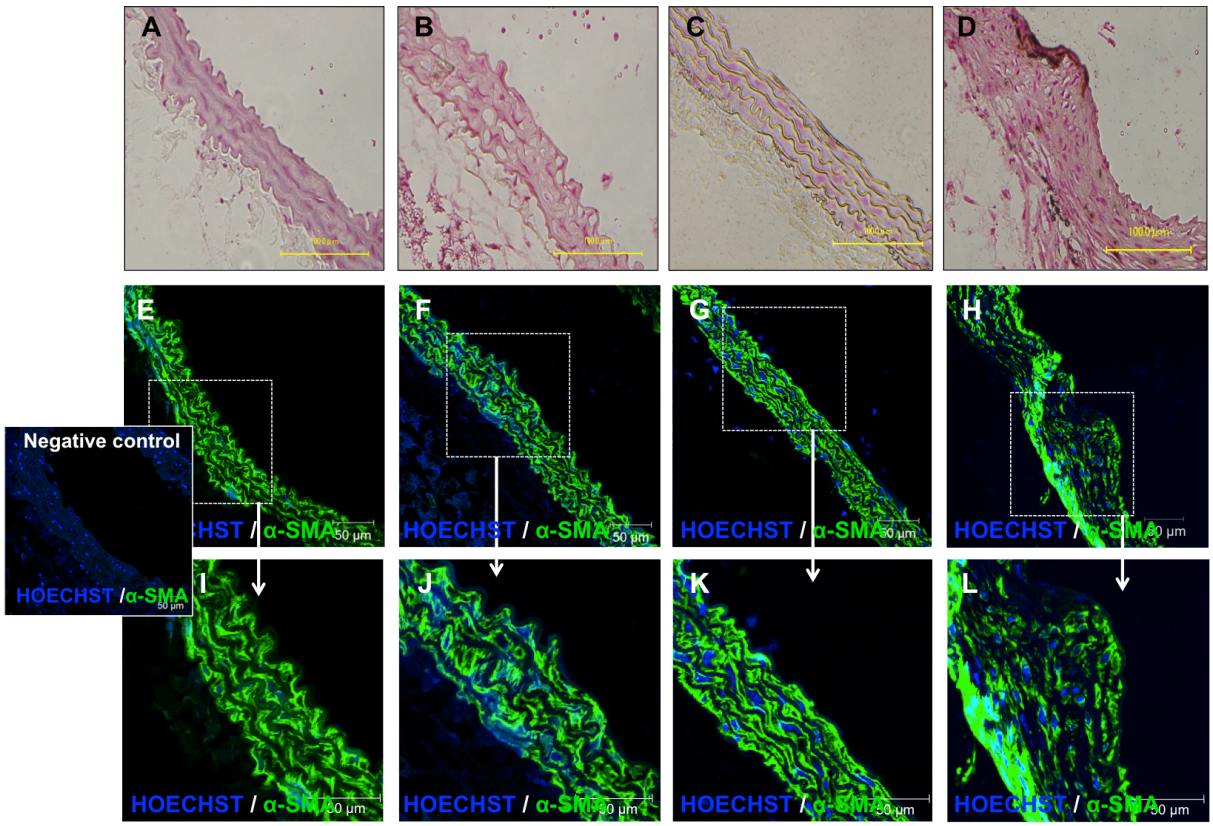

FIGURE 7

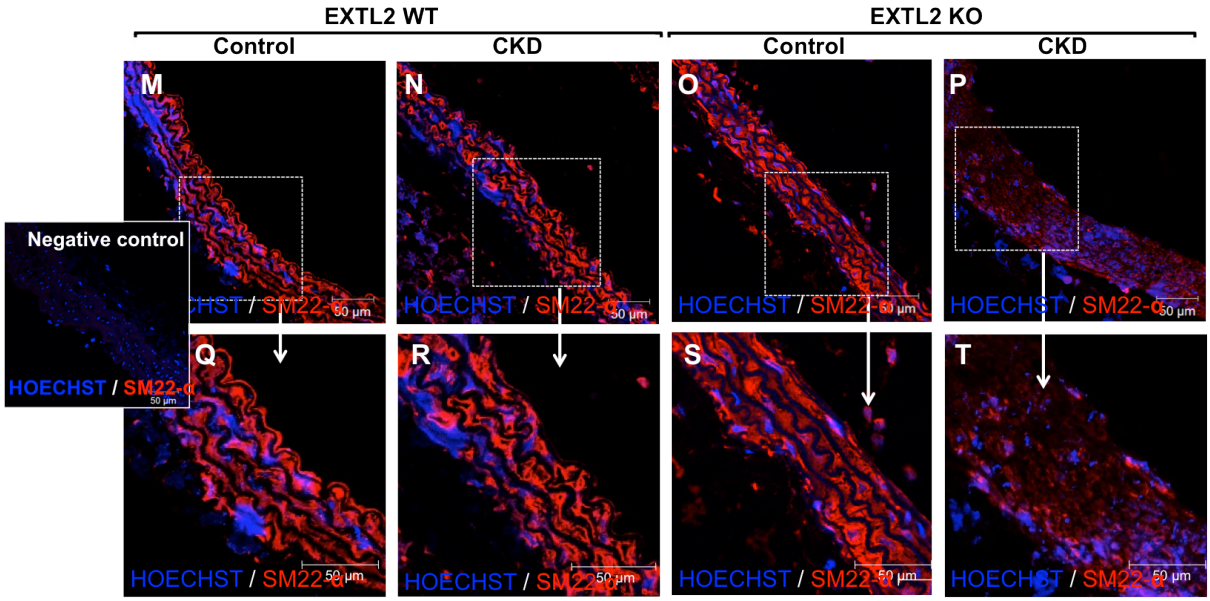
EXTL2 WT
EXTL2 KO
Control
CKD
Control
CKD
M
N
O
P
Negative control
HOECHST / SM22-α
50 μm
Q
R
S
T

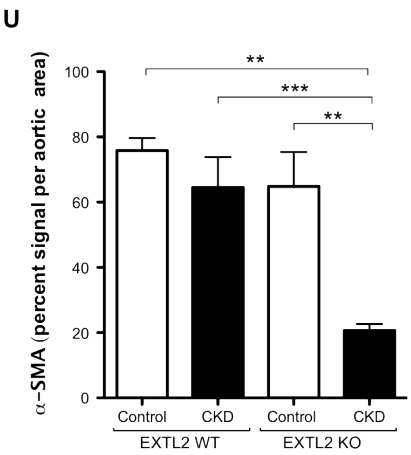
U
α–SMA (percent signal per aortic area)
100
80
60
40
20
0
**
***
**
Control
CKD
Control
CKD
EXTL2 WT
EXTL2 KO

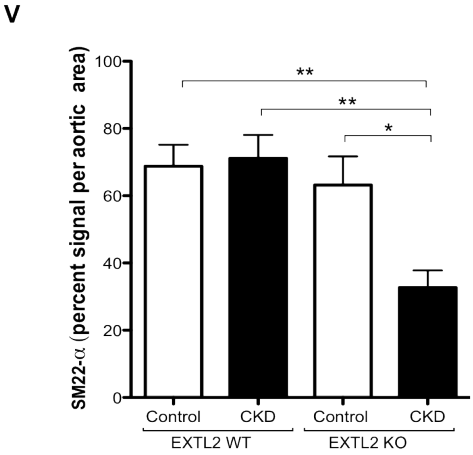
V
SM22-α (percent signal per aortic area)
100
80
60
40
20
0
**
**
*
Control
CKD
Control
CKD
EXTL2 WT
EXTL2 KO

FIGURE 8

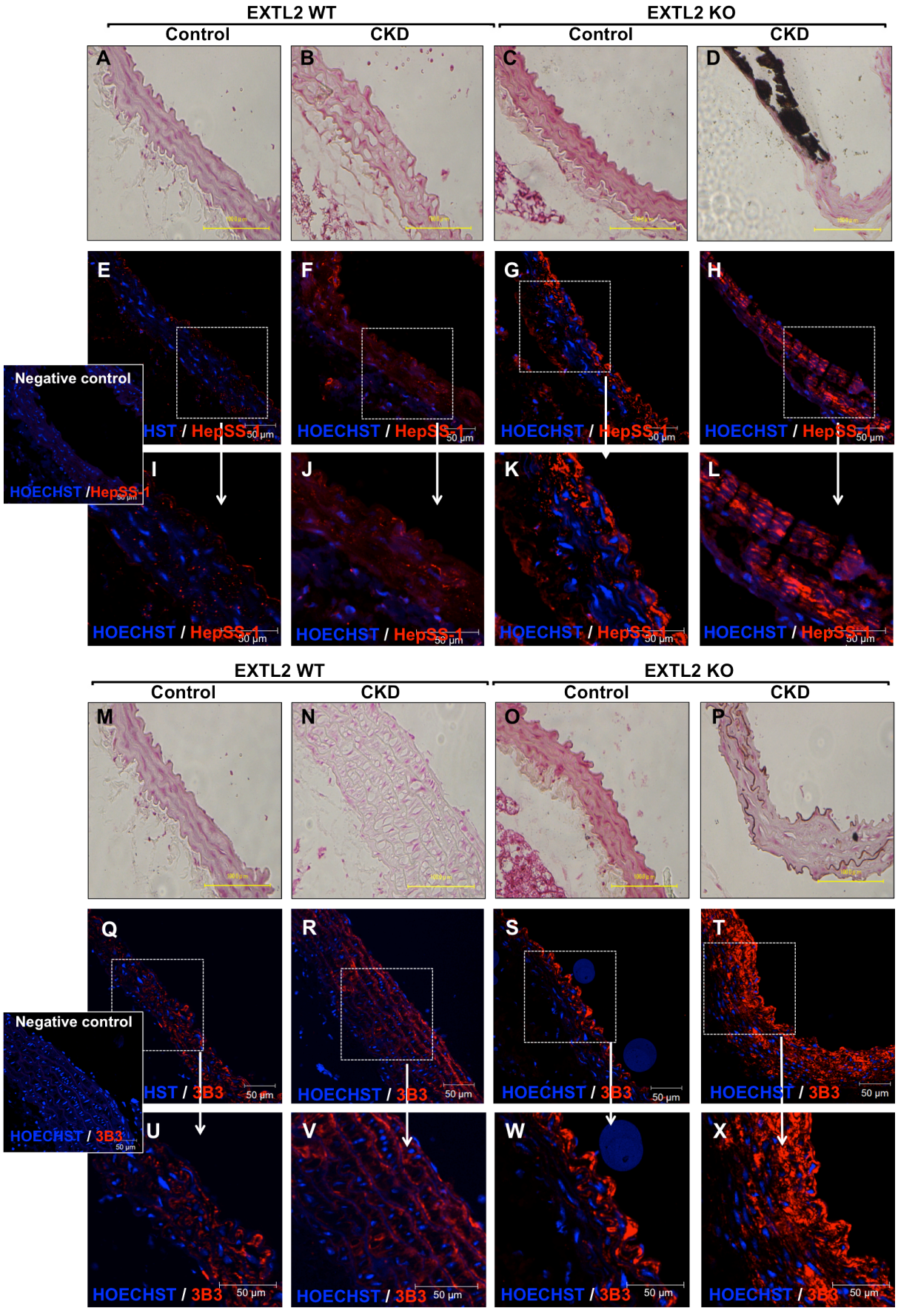
EXTL2 WT
EXTL2 KO
Control
CKD
Control
CKD
A
B
C
D
E
F
G
H
Negative control
HOECHST / HepSS-1
HOECHST / HepSS-1
HOECHST / HepSS-1
HOECHST / HepSS-1
HOECHST / HepSS-1
I
J
K
L
HOECHST / HepSS-1
HOECHST / HepSS-1
HOECHST / HepSS-1
HOECHST / HepSS-1
50 µm
EXTL2 WT
EXTL2 KO
Control
CKD
Control
CKD
M
N
O
P
Q
R
S
T
Negative control
HOECHST / 3B3
HOECHST / 3B3
HOECHST / 3B3
HOECHST / 3B3
HOECHST / 3B3
U
V
W
X
HOECHST / 3B3
HOECHST / 3B3
HOECHST / 3B3
HOECHST / 3B3
50 µm

FIGURE 8

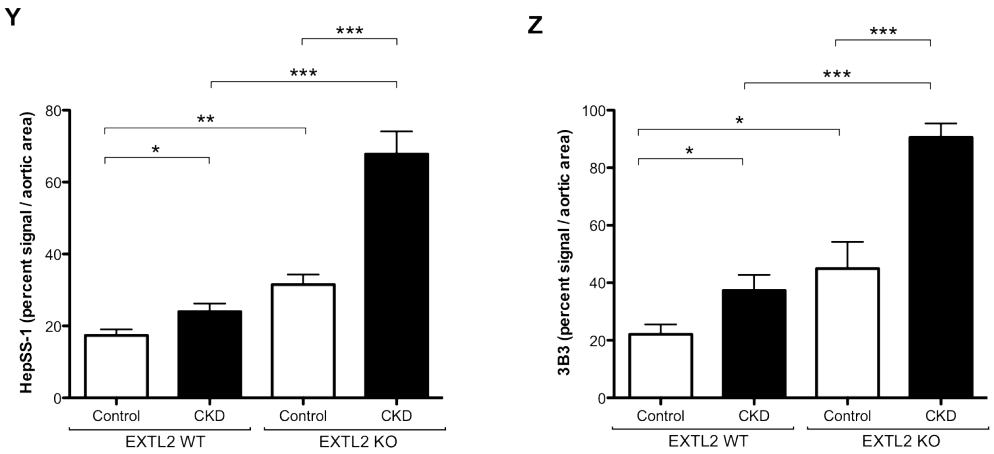

FIGURE 9

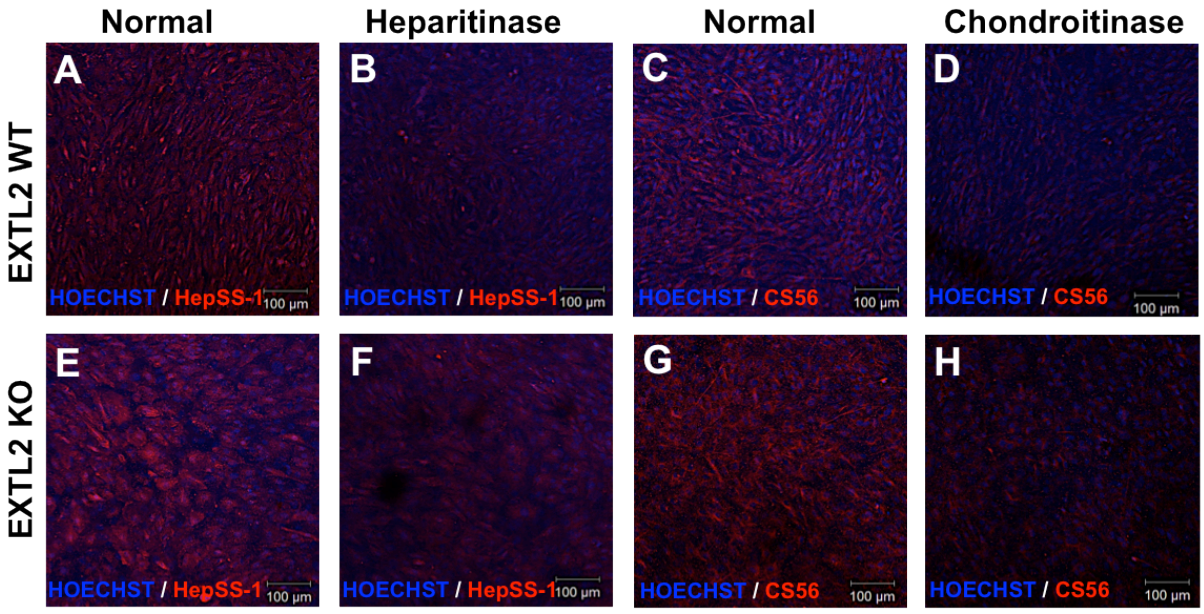

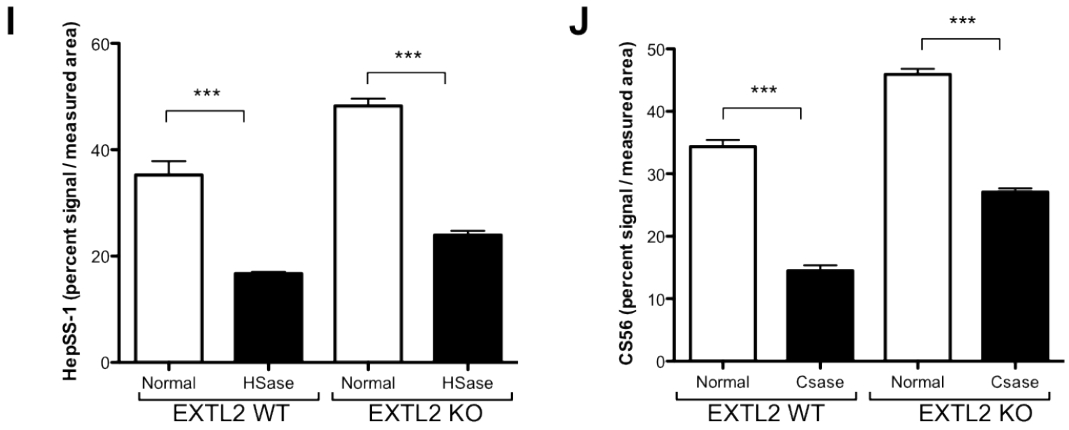

FIGURE 10

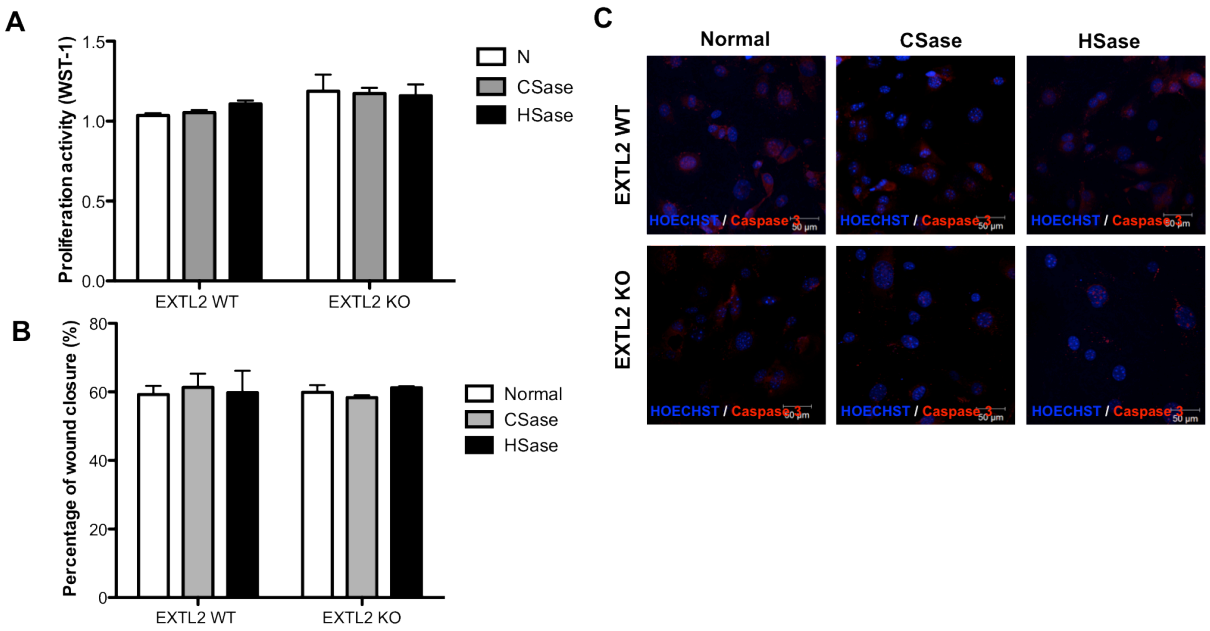
A
Proliferation activity (WST-1)
1.5
1.0
0.5
0.0
EXTL2 WT
EXTL2 KO
N
CSase
HSase
B
Percentage of wound closure (%)
80
60
40
20
0
EXTL2 WT
EXTL2 KO
Normal
CSase
HSase
C
Normal
CSase
HSase
EXTL2 WT
EXTL2 KO
HOECHST / Caspase-3
50 μm

FIGURE 11

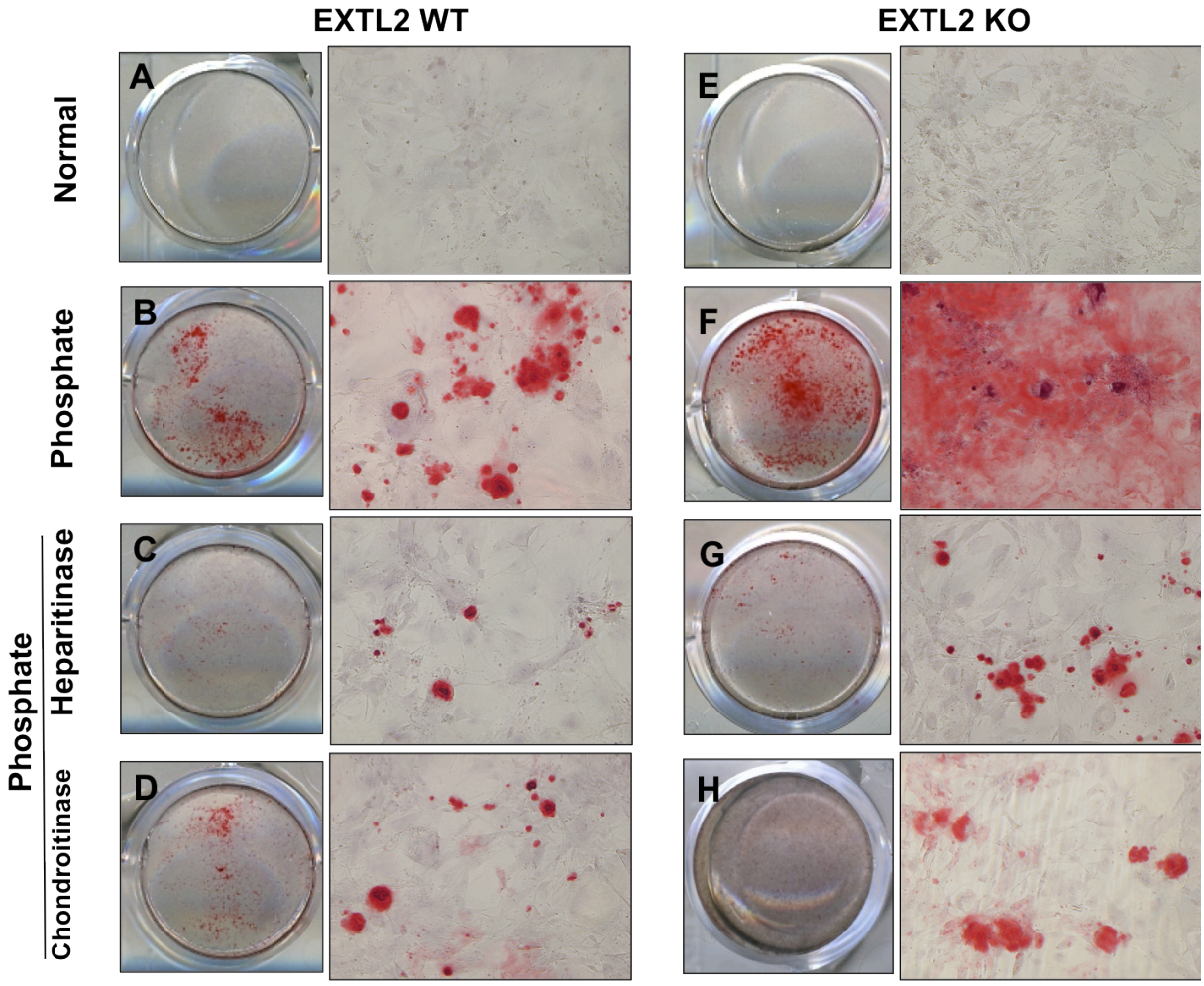
EXTL2 WT
EXTL2 KO
Normal
Phosphate
Phosphate
Heparitinase
Chondroitinase
A
B
C
D
E
F
G
H

I

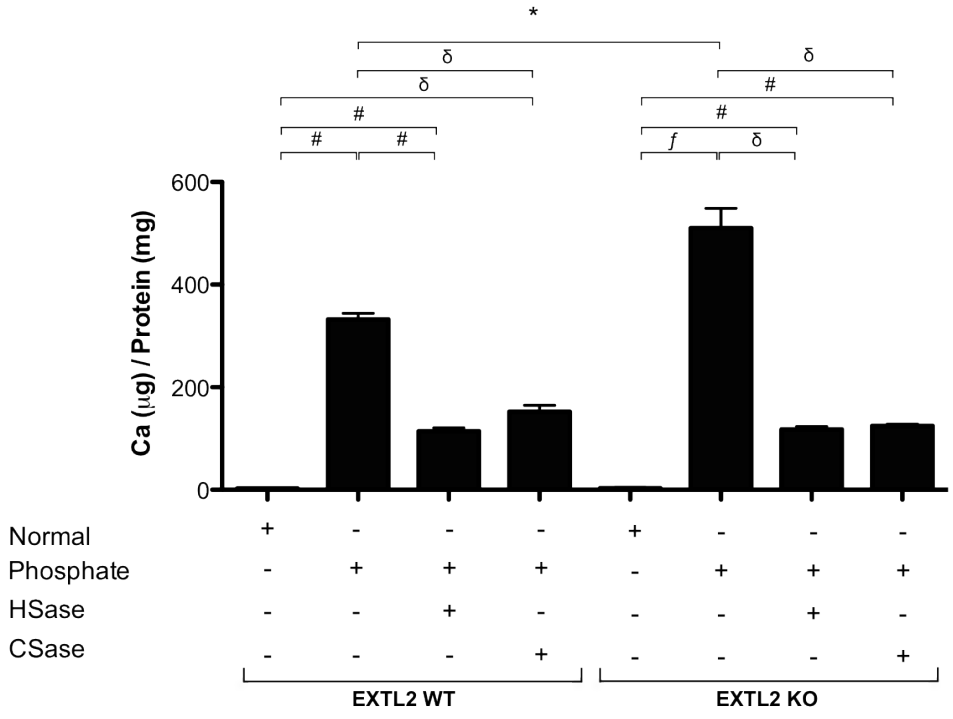
*
δ
δ
#
#
#
δ
#
#
f
δ
600
400
200
0
Ca (μg) / Protein (mg)
Normal
Phosphate
HSase
CSase
EXTL2 WT
EXTL2 KO

FIGURE 12

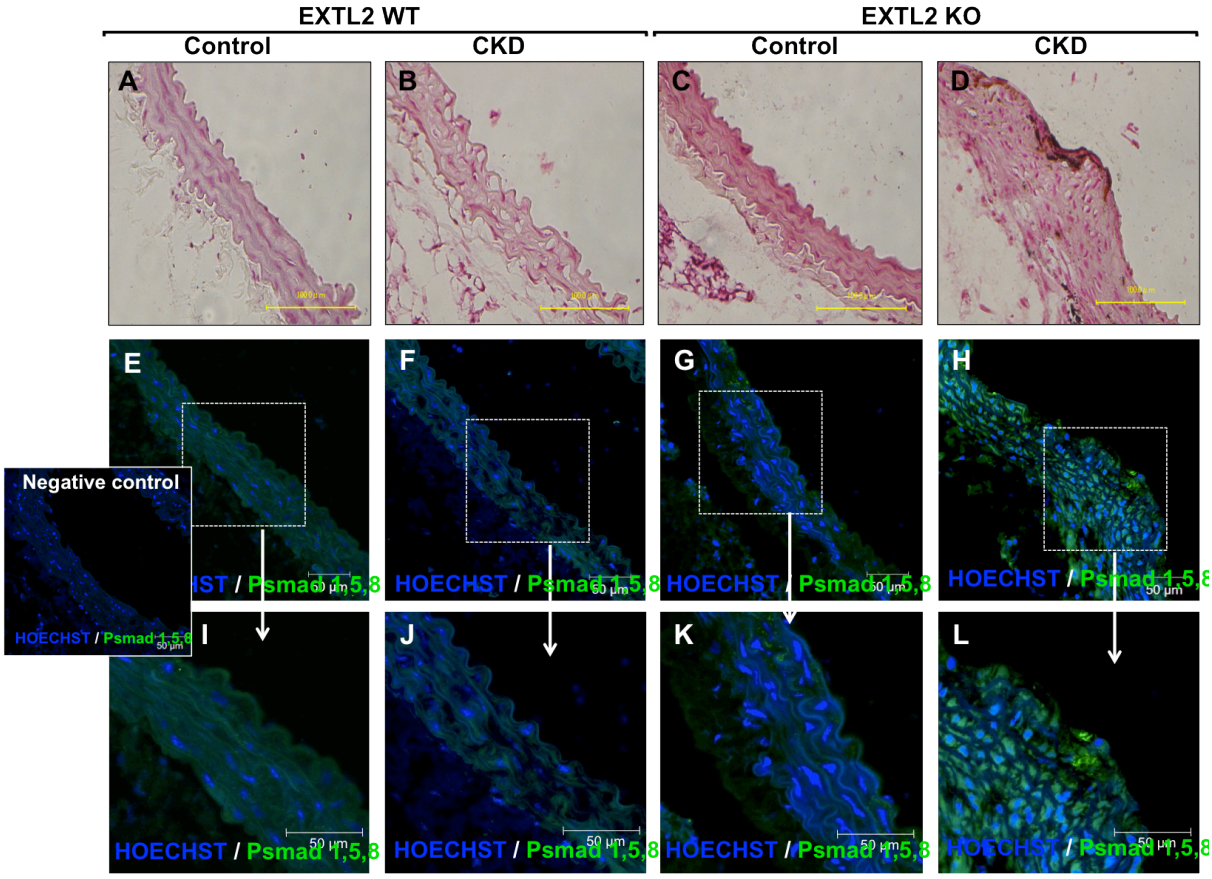
EXTL2 WT
EXTL2 KO
Control
CKD
Control
CKD
A
B
C
D
E
F
G
H
Negative control
HOECHST / Psmad 1,5,8
I
J
K
L
50 µm

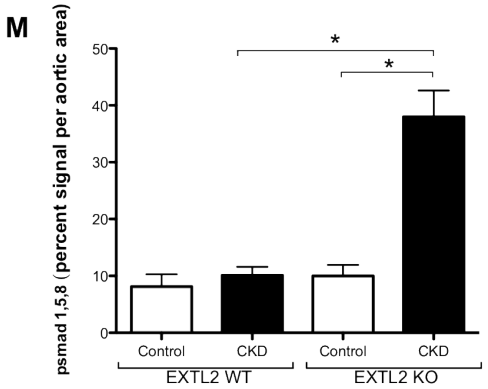
M
psmad 1,5,8 (percent signal per aortic area)
50
40
30
20
10
0
*
*
Control
CKD
Control
CKD
EXTL2 WT
EXTL2 KO

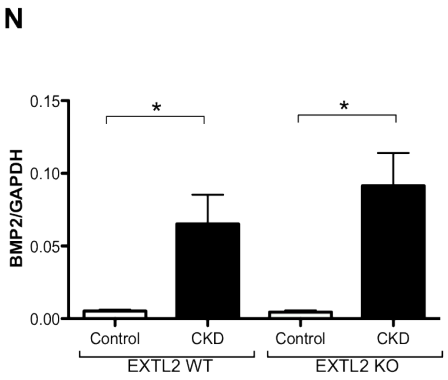
N
BMP2/GAPDH
0.15
0.10
0.05
0.00
*
*
Control
CKD
Control
CKD
EXTL2 WT
EXTL2 KO

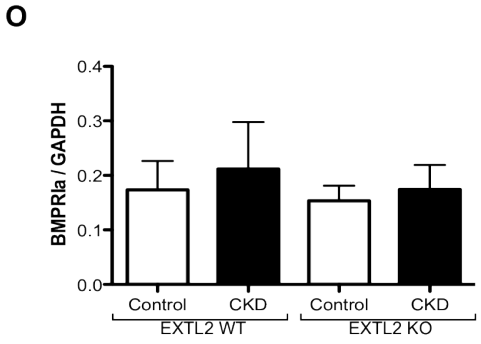
O
BMPRIa / GAPDH
0.4
0.3
0.2
0.1
0.0
Control
CKD
Control
CKD
EXTL2 WT
EXTL2 KO

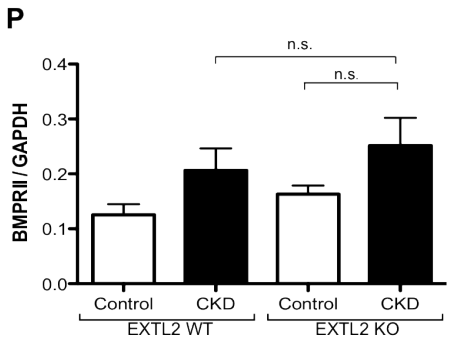
P
BMPRII / GAPDH
n.s.
n.s.
0.4
0.3
0.2
0.1
0.0
Control
CKD
Control
CKD
EXTL2 WT
EXTL2 KO

FIGURE 13

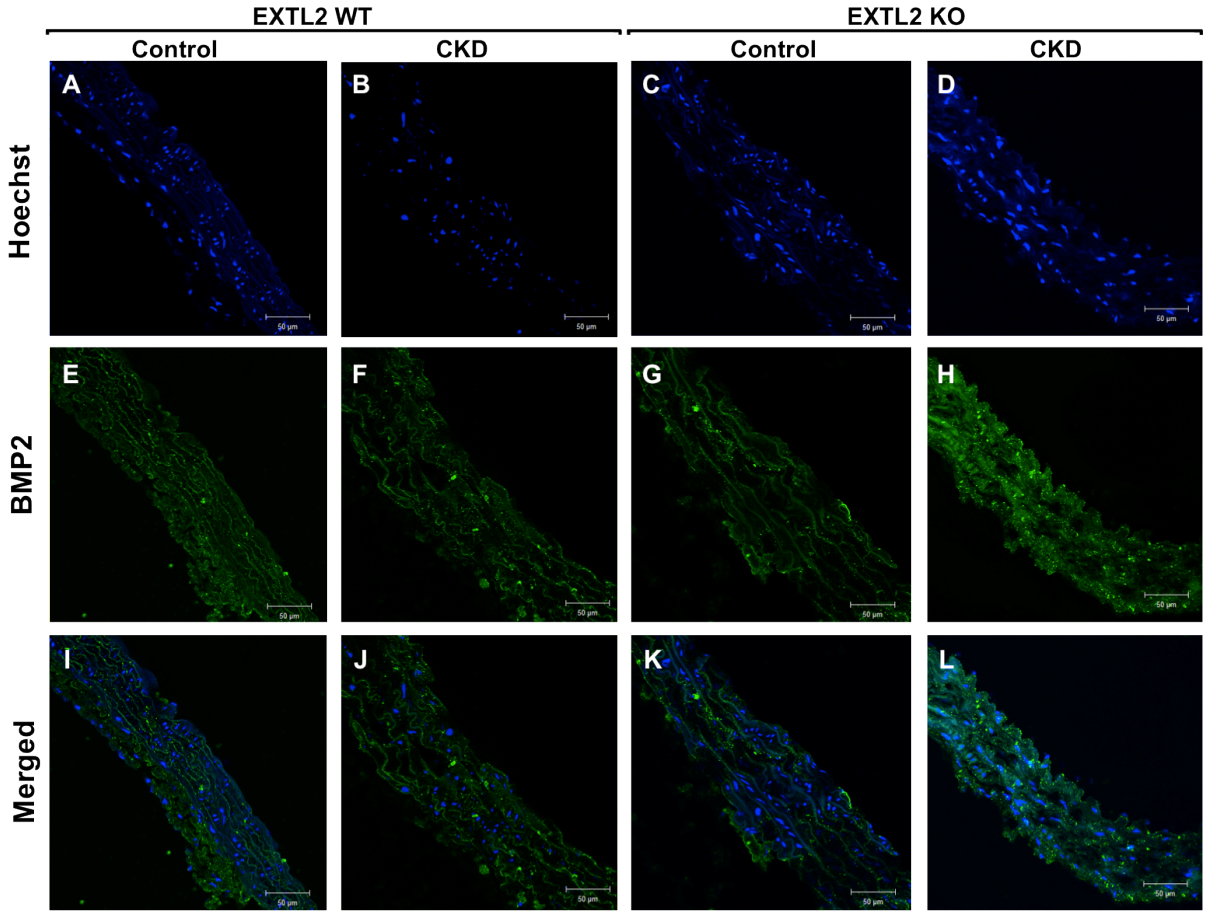
EXTL2 WT
EXTL2 KO
Control
CKD
Control
CKD
Hoechst
BMP2
Merged
A
B
C
D
E
F
G
H
I
J
K
L